

## Strongly Chemiluminescent Acridinium Esters under Neutral Conditions: Synthesis, Property, Determination and Theoretical Study

Manabu Nakazono, Yuji Oshikawa, Mizuho Nakamura, Hidehiro Kubota, and Shinkoh Nanbu

*J. Org. Chem.*, **Just Accepted Manuscript** • DOI: 10.1021/acs.joc.6b02748 • Publication Date (Web): 07 Feb 2017

Downloaded from <http://pubs.acs.org> on February 8, 2017

### Just Accepted

“Just Accepted” manuscripts have been peer-reviewed and accepted for publication. They are posted online prior to technical editing, formatting for publication and author proofing. The American Chemical Society provides “Just Accepted” as a free service to the research community to expedite the dissemination of scientific material as soon as possible after acceptance. “Just Accepted” manuscripts appear in full in PDF format accompanied by an HTML abstract. “Just Accepted” manuscripts have been fully peer reviewed, but should not be considered the official version of record. They are accessible to all readers and citable by the Digital Object Identifier (DOI®). “Just Accepted” is an optional service offered to authors. Therefore, the “Just Accepted” Web site may not include all articles that will be published in the journal. After a manuscript is technically edited and formatted, it will be removed from the “Just Accepted” Web site and published as an ASAP article. Note that technical editing may introduce minor changes to the manuscript text and/or graphics which could affect content, and all legal disclaimers and ethical guidelines that apply to the journal pertain. ACS cannot be held responsible for errors or consequences arising from the use of information contained in these “Just Accepted” manuscripts.

1  
2  
3  
4  
5  
6  
7 Strongly Chemiluminescent Acridinium Esters under Neutral  
8  
9  
10 Conditions: Synthesis, Property, Determination and Theoretical  
11  
12  
13  
14 Study  
15  
16  
17

18 *Manabu Nakazono,<sup>†,\*</sup> Yuji Oshikawa,<sup>†</sup> Mizuho Nakamura,<sup>‡</sup> Hidehiro Kubota<sup>§</sup>*

21 *and Shinkoh Nanbu<sup>‡</sup>*

22  
23  
24  
25 <sup>†</sup>Graduate School of Pharmaceutical Sciences, Kyushu University, 3-1-1 Maidashi, Higashi-ku,  
26 Fukuoka 812-8582, Japan  
27

28  
29  
30  
31 <sup>‡</sup>Faculty of Science and Technology, Sophia University, 7-1 Kioi-Cho, Chiyoda-ku, Tokyo 102-  
32 8554, Japan  
33

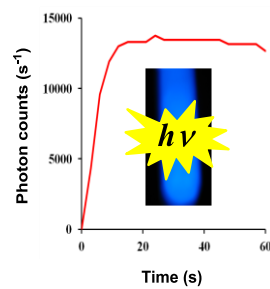
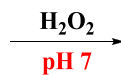
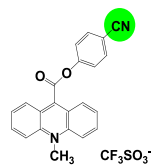
34  
35  
36  
37 <sup>§</sup>ATTO Corporation, 3-2-2 Motoasakusa, Taito-ku, Tokyo 111-0041, Japan  
38

39  
40  
41  
42  
43  
44 \*Corresponding author. Tel: +81-92-642-6597.

45  
46 E-mail address: nakazono@phar.kyushu-u.ac.jp.  
47  
48  
49  
50  
51  
52  
53  
54  
55  
56  
57  
58  
59  
60

## Table of Contents

Electron-withdrawing group



**ABSTRACT**

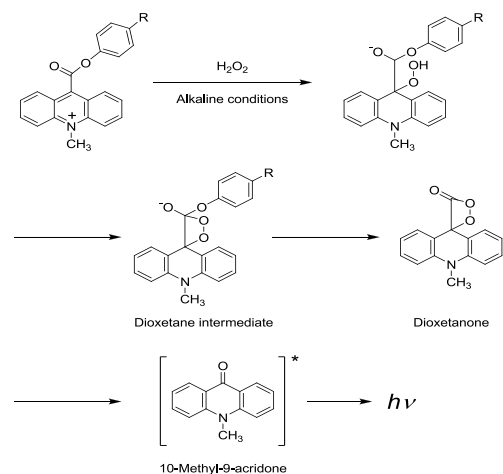
Various novel acridinium ester derivatives having phenyl and biphenyl moieties were synthesized and their optimal chemiluminescence conditions were investigated. Several strongly chemiluminescent acridinium esters under neutral conditions were found and then these derivatives were used to detect hydrogen peroxide and glucose. Acridinium esters having strong electron-withdrawing groups such as cyano, methoxycarbonyl and nitro groups at the 4-position of the phenyl moiety in phenyl 10-methyl-10 $\lambda^4$ -acridine-9-carboxylate, trifluoromethanesulfonate salt showed strong chemiluminescence intensities. The chemiluminescence intensity of 3,4-dicyanophenyl 10-methyl-10 $\lambda^4$ -acridine-9-carboxylate, trifluoromethanesulfonate salt was approximately 100 times stronger than that of phenyl 10-methyl-10 $\lambda^4$ -acridine-9-carboxylate, trifluoromethanesulfonate salt at pH 7. The linear calibration ranges of hydrogen peroxide and glucose were 0.05–10 mM and 10–2000  $\mu$ M using 3,4-(dimethoxycarbonyl)phenyl 10-methyl-10 $\lambda^4$ -acridine-9-carboxylate, trifluoromethanesulfonate salt at pH 7 and pH 7.5, respectively. The proposed chemiluminescence reaction mechanism of acridinium ester via a dioxetanone structure was evaluated via quantum chemical calculation on density functional theory. The proposed mechanism was composed of the nucleophilic addition reaction of hydroperoxide anion, the dioxetanone ring formation and nonadiabatic transition due to spin-orbit coupling around the transition state (TS) to the triplet state ( $T_1$ ) following the decomposition pathway. The TS which appeared in the thermal decomposition would be a rate-determining step for all three processes.

**KEYWORDS:** chemiluminescence, acridinium ester, hydrogen peroxide, glucose, neutral condition

## INTRODUCTION

Chemiluminescence (CL) assays have been utilized for determining various kinds of compounds qualitatively and quantitatively.<sup>1-11</sup> CL compounds have been developed as useful luminescent reagents. In particular, luminol (3-aminophthalhydrazide) derivatives,<sup>12-21</sup> acridinium ester derivatives<sup>22-30</sup> and dioxetane derivatives<sup>31-37</sup> are essential compounds in highly sensitive CL assays. Recently, luminol was applied to CL imaging in vivo by CL resonance energy transfer (CRET).<sup>38</sup> Acridinium ester derivatives have been frequently selected in enzyme immunoassays.<sup>39-41</sup> Intramolecular chemically initiated electron exchange luminescence mechanism and CRET were applied to acridinium-substituted 1,2-dioxetanes.<sup>42</sup> CL sensing of fluoride ions using a self-immolation mechanism was developed based on dioxetane CL.<sup>43</sup> The CL property and mechanism of 2-coumaranones were clarified by experimental and theoretical study.<sup>44</sup>

Acridinium esters react with hydrogen peroxide to produce fluorescent 10-methyl-9-acridone via a dioxetanone structure (Scheme 1).<sup>45,46a</sup> Acridinium ester derivatives have relatively strong CL intensity among CL compounds and various derivatives can be synthesized in a facile manner. 10-Carboxymethylacridinium derivatives were synthesized, when methyl group (an electron-donating group) was introduced at the 2 and 6-position of the phenyl moiety, strong CL intensity was obtained.<sup>23</sup> 9-Acridine carboxylic esters of hydroxamic and sulphohydroxamic acids had strong CL intensity at pico molar levels.<sup>25</sup> Acridinium dimethylphenyl esters containing *N*-sulfopropyl groups in the acridinium ring were highly sensitive CL compounds.<sup>39b</sup> 2',6'-dimethyl-4'-(*N*-succinimidylcarbonyl)phenyl-10-methyl-acridinium-9-carboxylate-1-

**Scheme 1.** Chemiluminescence mechanism of acridinium esters.

propanesulfonate inner salt was used for capillary CL determination of sympathomimetic drugs.<sup>47</sup> These CL compounds were dissolved in acetonitrile or dimethylformamide, the CL was measured in sodium hydroxide and hydrogen peroxide solution. In general, most CL compounds require strong alkaline conditions and the CL signals are short lasting. A little was studied about acridinium esters having novel CL property under neutral conditions. Di-*ortho*-bromophenyl acridinium ester generated CL signal under neutral conditions.<sup>48,49</sup> If compounds exhibiting strong CL under neutral conditions could be identified, it would be possible to develop novel and useful CL assays. For example, in the CL measurement of an enzyme activity producing hydrogen peroxide under neutral conditions, the enzyme activity could be measured without the addition of alkali. Therefore, a method is needed to synthesize acridinium esters that can readily react with hydrogen peroxide under neutral conditions. In a previous study, the introduction of electron-withdrawing groups such as bromide to the 4-position of the phenyl moiety in phenyl 10-methyl-10 $\lambda^4$ -acridine-9-carboxylate, trifluoromethanesulfonate salt was shown to increase the CL intensity of acridinium esters.<sup>46a</sup> Electron-withdrawing groups could polarize the electron

1  
2  
3 density toward the phenyl ring and thereby reduce the electron density at the C9 position of the  
4 acridine moiety. Hydroperoxide anion ( $\text{HOO}^-$ ) reacts with the C9 position in a facile manner and  
5 light is produced.<sup>46a</sup> First, therefore, we decided to focus on cyano, trifluoromethyl,  
6 methoxycarbonyl and nitro groups. We thus considered that the detailed effects of electron-  
7 donating groups and electron-withdrawing groups on the 4-position of the phenyl moiety in  
8 phenyl 10-methyl-10 $\lambda^4$ -acridine-9-carboxylate, trifluoromethanesulfonate salt should also be  
9 evaluated. In a related experiment, we investigated the increase of CL intensity by the increase  
10 of acridinium moieties. Second, the crystal structure of [1,1'-biphenyl]-4-yl 10-methyl-10 $\lambda^4$ -  
11 acridine-9-carboxylate, trifluoromethanesulfonate salt was previously cleared and the two phenyl  
12 rings of the biphenyl moiety was oriented at a dihedral angle of 42.9°.<sup>50</sup> We predicted that the  
13 twist structure of the biphenyl moiety would cause rapid cleavage of the biphenoxy moiety in the  
14 dioxetane intermediate, and thereby increase the production of 10-methyl-9-acridone and the  
15 level of CL intensity. Thus, various derivatives of [1,1'-biphenyl]-4-yl 10-methyl-10 $\lambda^4$ -acridine-  
16 9-carboxylate, trifluoromethanesulfonate salt were synthesized.

17  
18  
19  
20  
21  
22  
23  
24  
25  
26  
27  
28  
29  
30  
31  
32  
33  
34  
35  
36  
37 Useful CL methods for determining various analytes are developed by measurement of  
38 enzymatically generated hydrogen peroxide. For example, glucose reacts with glucose oxidase  
39 (EC1.1.3.4) in the presence of oxygen, and hydrogen peroxide is generated. The quantification  
40 of glucose can be achieved by the reaction of hydrogen peroxide and CL compound. In this  
41 study, various novel acridinium ester derivatives were designed and synthesized, and their CL  
42 was measured. Finally, novel acridinium esters, which appear to have strong CL intensity under  
43 neutral conditions, were developed and utilized for the CL determination of hydrogen peroxide  
44 and glucose. Furthermore, a theoretical study was performed to clarify the charge distributions  
45  
46  
47  
48  
49  
50  
51  
52  
53  
54  
55  
56  
57  
58  
59  
60

of C9 and N10 positions of acridine moiety and energy diagram on the proposed CL mechanism by *ab initio* chemical calculations.

## RESULTS and DISCUSSION

**Synthesis of Compounds 1–26.** Acridine-9-carbonyl chloride and biphenols were prepared by previously described methods.<sup>51,52</sup> The esterification reaction of acridine-9-carbonyl chloride

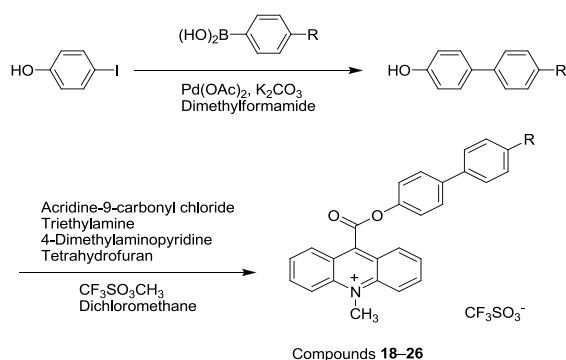
**Table 1.** Synthesis and chemical structure of compounds 1–17.

Compounds 1–17

Compound	R	Yield (%)	Compound	R	Yield (%)
1		13	10		4
2		14	11		46
3		23	12		12
4		13	13		13
5		25	14		23
6		63	15		50
7		26	16		4
8		57	17		21
9		30			

and phenols proceeded promisingly in the presence of triethylamine, 4-dimethylaminopyridine and tetrahydrofuran. Methyl trifluoromethanesulfonate was used for the *N*-methylation of acridine moieties in dichloromethane (Table 1). As shown in Table 2, 4-iodophenol was transformed by arylboronic acids through Suzuki-Miyaura coupling and compounds **18–20** were synthesized in a facile manner. In the synthesis of compound **26**, 1,1':4',1''-terphenyl-4-ol was prepared by 4-bromo-4'-hydroxyphenyl and phenylboronic acid in the presence of tetrakis(triphenylphosphine)palladium, potassium carbonate and dimethoxyethane.<sup>53</sup> In the purification of compounds **1–26** by column chromatography, the crude products were excluded by chloroform-methanol solution (v/v, 20/1) and compounds **1–26** were eluted by using chloroform-methanol solution (v/v, 5/1, 4/1 or 2/1).

**Table 2.** Synthesis and chemical structure of compounds **18–26**.



Compound	R	Yield (%)
<b>18</b>	CH <sub>3</sub>	33
<b>19</b>	CH <sub>2</sub> CH <sub>3</sub>	5
<b>20</b>	OCH <sub>3</sub>	12
<b>21</b>	Br	29
<b>22</b>	COOCH <sub>3</sub>	11
<b>23</b>	COOCH <sub>2</sub> CH <sub>3</sub>	20
<b>24</b>	COOBn	9
<b>25</b>	NO <sub>2</sub>	45
<b>26</b>	Ph	6

**Chemiluminescence Property of Compounds 1–26.** Compounds **3**, **4** and **9–13** had particularly strong CL intensities at pH 7. The CL of compounds **3** and **10–13** was long-lasting.

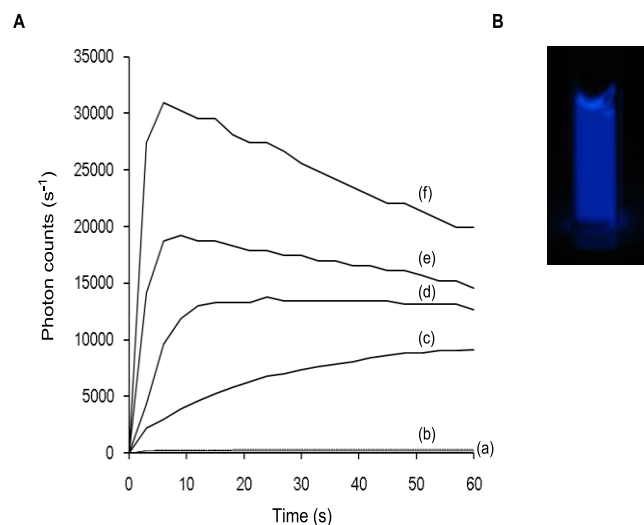


**Figure 1.** (A) Time-course of the chemiluminescence development of compounds **1**, **3**, **9**, **12**, **13** and luminol in 100 mM Tris-HCl buffer at pH 7: (a) luminol (b) compound **1** (c) compound **9** (d) compound **3** (e) compound **13** (f) compound **12**. The concentration of compounds **1**, **3**, **9**, **12**, **13** and luminol was 10 nM. The concentration of hydrogen peroxide was 5 mM. (B) Chemiluminescence of compound **3** (100  $\mu$ M) in 100 mM phosphate buffer at pH 7.

In compound **3**, the time required to the maximum photon count was 15 s after the addition of hydrogen peroxide (Figure 1A). In contrast, the CL intensities of compound **1** and luminol were very weak at pH 7. Compared to the CL curves of compounds **3**, **9**, **12** and **13**, increasing the number of electron-withdrawing groups on the phenyl moiety caused the increase of CL intensity. Compound **3** produced CL in phosphate buffer at pH 7 and blue light emission was observed (Figure 1B). The effect of pH on the CL development of compounds **1–17** is shown in Figure 2.

Novel acridinium esters that can produce strong CL were found under neutral conditions (pH 7 and pH 8). Most of compounds **1–17** had maximum CL intensities at pH 8. However, the CL

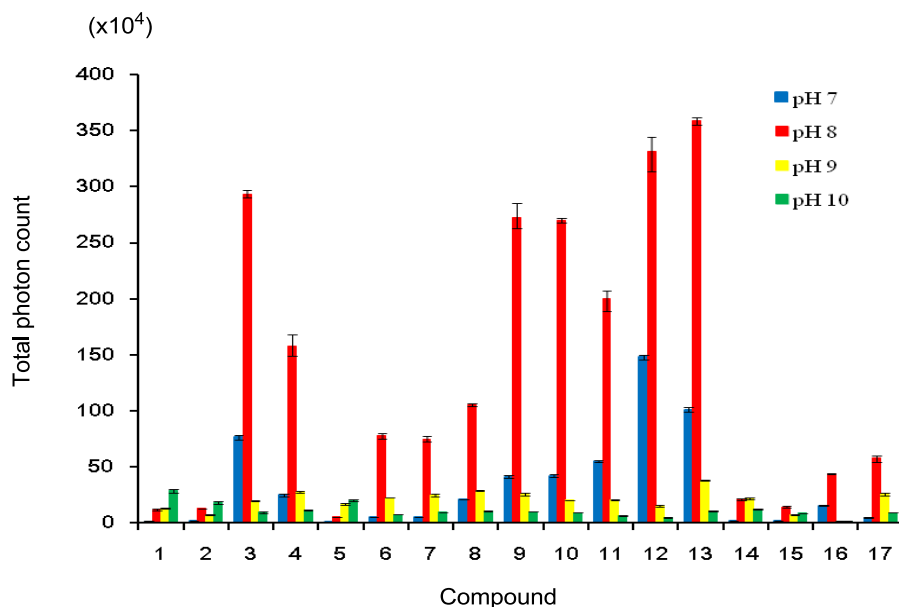


**Figure 2.** Effect of pH on the chemiluminescence development of compounds **1–17**. To 10 nM solution of compounds **1–17** in dimethyl sulfoxide was added buffer solution (100 mM Tris-HCl for pH 7 and pH 8, 100 mM Gly-NaOH for pH 9 and pH 10). The CL reaction was initiated by adding 5 mM aqueous hydrogen peroxide solution to the luminometer. The CL emission was measured for 1 min and the integral photon counts were used to evaluate the CL intensity.

intensities of compounds **1** and **5** increased under alkaline conditions (pH 9 and pH 10). In compounds **2–17**, the CL intensities appeared to be greater than that of compound **1** at pH 7 (Figure 3). The CL intensity of compound **12** was approximately 100 times stronger than that of

compound **1** at pH 7. The introduction of strong electron-withdrawing groups such as cyano, methoxycarbonyl and nitro groups at the 4-position of the phenyl moiety increased the CL intensity and that of electron-donating groups such as methyl and methoxy groups decreased the CL intensity. Quantum yields of acridinium esters are correlated with the pKa of the leaving

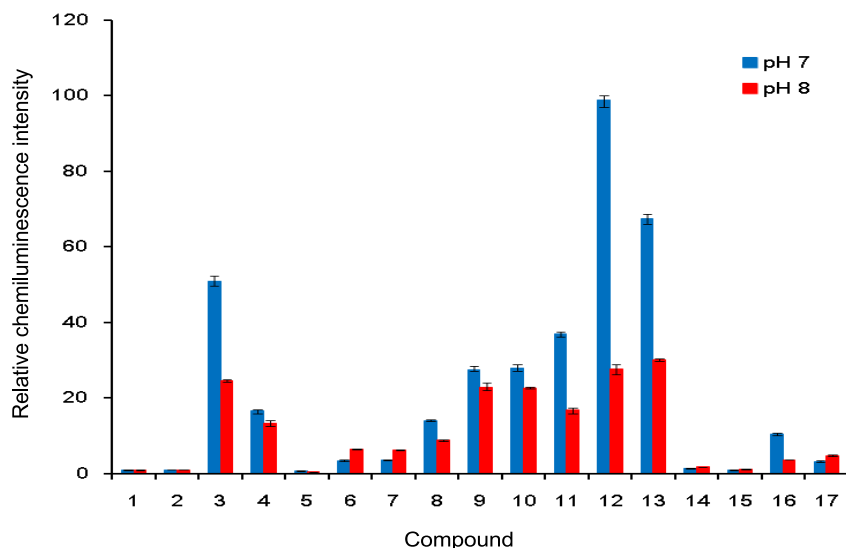


**Figure 3.** Relative chemiluminescence intensity of compounds **1–17** at pH 7 and pH 8. The concentration of compounds **1–17** was 10 nM. The concentration of hydrogen peroxide was 5 mM. Chemiluminescence was measured for 1 min. The CL intensity of compound **1** at each pH 7 and pH 8 was taken as 1.

group.<sup>54</sup> The pKa values of phenols having electron-withdrawing groups at 4-position of phenol moiety are 7.1–8.5.<sup>55</sup> When electron-withdrawing groups to the 4-position of the phenyl moiety are introduced, the pKa of the leaving group decreases.<sup>55</sup> Based on the CL mechanism of acridinium ester (Scheme 1), probably the phenyl moiety of compounds **3**, **4** and **8–13** is readily left and 10-methyl-9-acridone is produced. In 100 mM phosphate buffer (pH 7), the relative CL



1  
2  
3 of a methoxycarbonyl (compound **22**) and a nitro group (compound **25**) at the 4-position of the  
4 biphenyl moiety caused an increase of CL intensity (Figure S3 in supporting information). The  
5 CL intensity of compound **25** at pH 8 was approximately 5 times stronger than that of compound  
6  
7  
8  
9  
10 **14**. Unfortunately, the CL intensity of compound **26** did not increase (Table S1 in supporting  
11 information). Taken together, these results demonstrate that the introduction of electron-  
12 withdrawing groups to the 4-position of the phenyl and biphenyl moieties is crucial for  
13 increasing the CL intensity of acridinium esters.  
14  
15  
16  
17  
18  
19

### 20 **Standard Curves for Hydrogen Peroxide at pH 7 and pH 8 using Compounds 3, 4 and 13.**

21 Compounds **3**, **4** and **13** having high chemical stability were used for determination of hydrogen  
22 peroxide. The CL intensities of compounds **1–17** increased with the increase of hydrogen  
23 peroxide concentration (5–100 mM) at pH 7. Standard curves for hydrogen peroxide at pH 7  
24 and pH 8 using compounds **3**, **4** and **13** were shown in Figure 5. The linear calibration ranges of  
25 hydrogen peroxide were 0.05–25 mM (regression equation:  $y = 121812x + 68861$ ,  $R=0.997$ ) at  
26 pH 7 and 0.05–5 mM (regression equation:  $y = 613613x + 126736$ ,  $R=0.996$ ) at pH 8 using  
27 compound **3**. The relative standard deviation was mostly within 4.8% ( $n=3$ ). The detection  
28 limits ( $S/N=2$ ) of hydrogen peroxide were 50  $\mu\text{M}$  at pH 7 and pH 8, respectively. The linear  
29 calibration ranges of hydrogen peroxide were 0.1–40 mM (regression equation:  $y = 33036x +$   
30  $52387$ ,  $R=0.997$ ) at pH 7 and 0.05–5 mM (regression equation:  $y = 340474x + 41759$ ,  $R=0.999$ )  
31 at pH 8 using compound **4**. The relative standard deviation was mostly within 5.8% ( $n=3$ ). The  
32 detection limits ( $S/N=2$ ) of hydrogen peroxide were 100  $\mu\text{M}$  at pH 7 and 50  $\mu\text{M}$  at pH 8. The  
33 linear calibration ranges of hydrogen peroxide were 0.05–10 mM (regression equation:  $188851x$   
34  $+ 12236$ ,  $R=0.999$ ) at pH 7 and 0.025–1 mM (regression equation:  $y = 1120300x + 21398$ ,  
35  
36  
37  
38  
39  
40  
41  
42  
43  
44  
45  
46  
47  
48  
49  
50  
51  
52  
53  
54  
55  
56  
57  
58  
59  
60

R=0.999) at pH 8 using compound **13**, respectively. The relative standard deviation was mostly within 4.3% (n=3). The detection limits ( $S/N=2$ ) of hydrogen peroxide were 50  $\mu\text{M}$  at pH 7 and

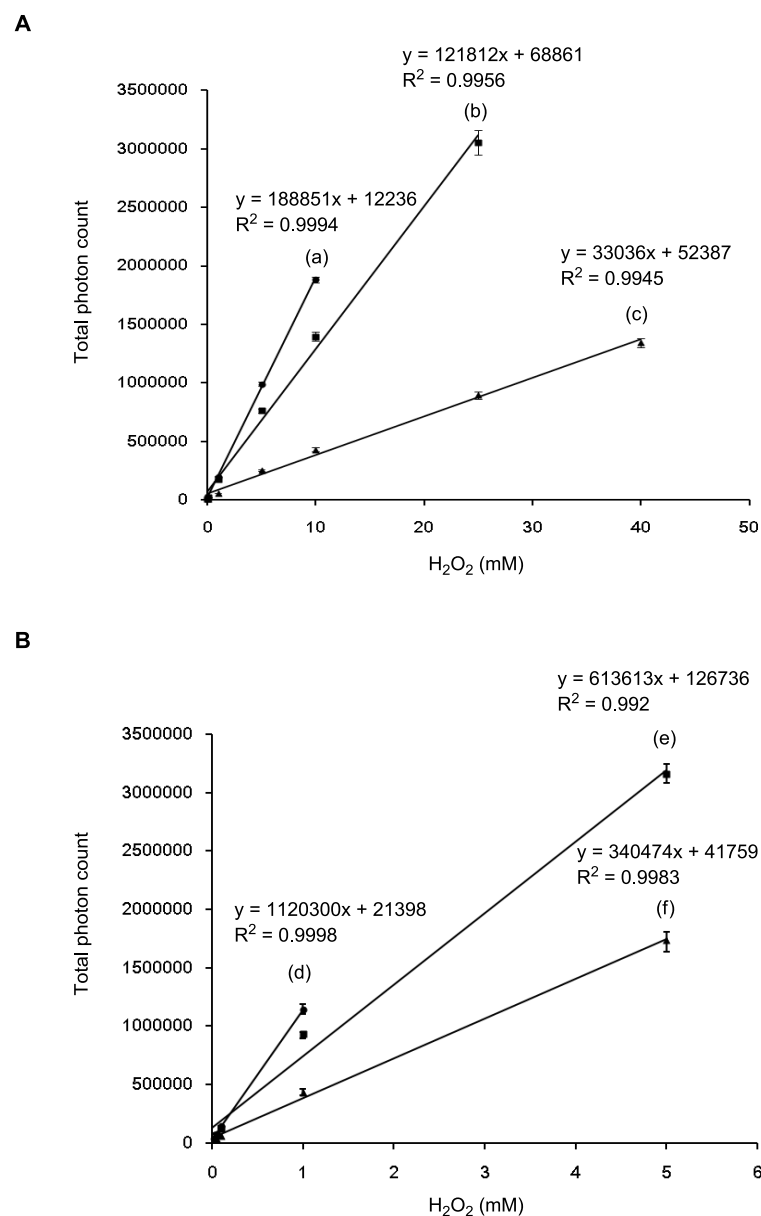
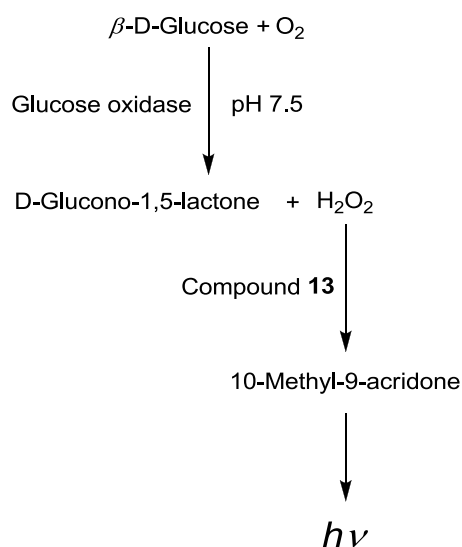


**Figure 5.** Standard curves of hydrogen peroxide in 100 mM Tris-HCl buffer at pH 7 and pH 8 using compounds **3**, **4** and **13**: (A) pH 7 (a) compound **13** (b) compound **3** (c) compound **4** (B) pH 8 (d) compound **13** (e) compound **3** (f) compound **4**. The concentration of compounds **3**, **4** and **13** was 10 nM. Chemiluminescence was measured for 1 min.

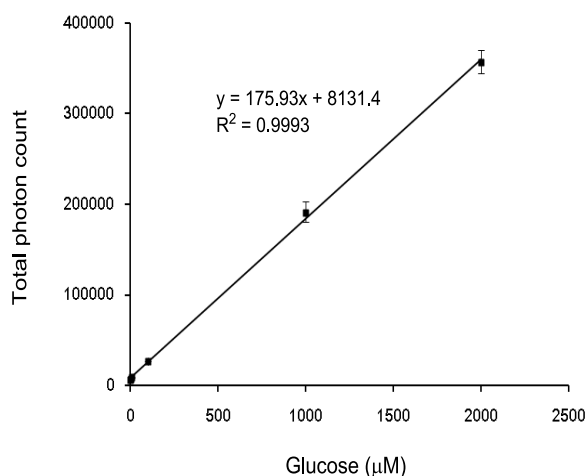
25  $\mu\text{M}$  at pH 8, respectively. A long range of detectability and satisfactory reproducibility for the detection of hydrogen peroxide were obtained at pH 7 and pH 8. Similar standard curves were obtained at pH 7 and pH 8 in 100 mM phosphate buffer (Figure S5 in supporting information). In particular, the linear calibration ranges of hydrogen peroxide were 0.01–5 mM ( $R=0.993$ ) at pH 7 and 5–1000  $\mu\text{M}$  ( $R=0.999$ ) at pH 8 using compound **13**, respectively. The relative standard deviation was mostly within 5.4% ( $n=3$ ). The detection limits ( $S/N=2$ ) of hydrogen peroxide were 10  $\mu\text{M}$  at pH 7 and 5  $\mu\text{M}$  pH 8, respectively. Compounds **3**, **4** and **13** were thus shown to be suitable for the CL determination of hydrogen peroxide under neutral conditions.

**Standard Curves for Glucose using Compound 13.** Compound **13** was very stable, used for the determination of hydrogen peroxide and applied for highly sensitive detection of glucose (Scheme 2). The linear calibration range of glucose was 10–2000  $\mu\text{M}$  (regression equation:  $y =$

**Scheme 2.** Chemiluminescence determination of glucose using compound **13** at pH 7.5.



1  
2  
3 175.93x + 8131.4, R=0.999) at pH 7.5 using compound **13** (Figure 6). The relative standard  
4 deviation was mostly within 4.1% (n=3). The detection limit (defined as the mean value of blank  
5 + 5 $\sigma$ ) of glucose was 5  $\mu$ M. This CL method of glucose showed similar sensitivity and linearity  
6 compared to the previous CL methods such as 1-ethyl-3-methylimidazolium ethylsulfate/Cu<sup>2+</sup>-  
7 luminol-glucose oxidase, luminol-H<sub>2</sub>O<sub>2</sub>-horseradish peroxidase-glucose oxidase and the Cu<sup>II</sup>-  
8 catalyzed CL of lucigenin using synthetic imidazolium-based ionic liquid derivatives.<sup>57-59</sup> Thus,  
9 this CL method can detect glucose at relatively high sensitivity without the addition of alkali and  
10 catalyst.  
11  
12  
13  
14  
15  
16  
17  
18  
19  
20  
21  
22  
23  
24

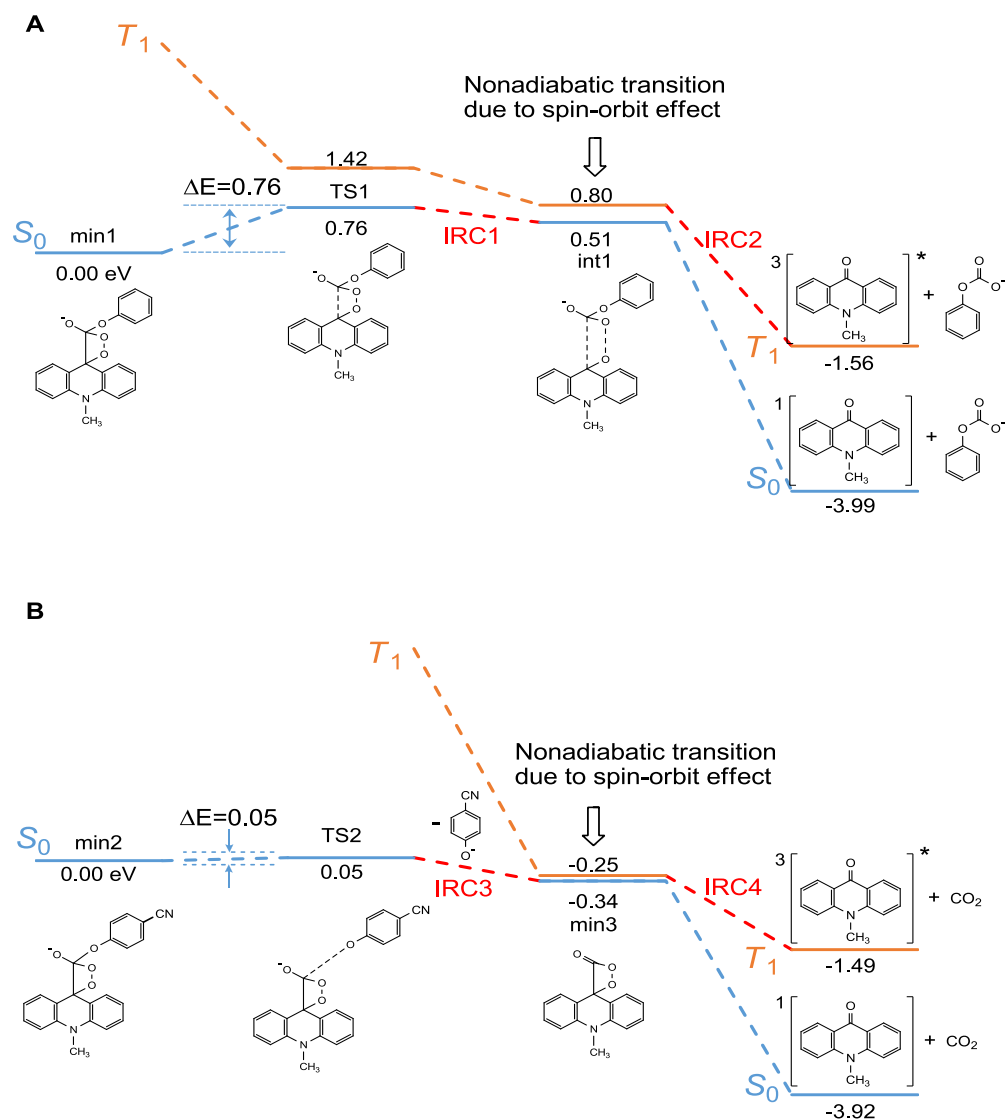


25  
26  
27  
28  
29  
30  
31  
32  
33  
34  
35  
36  
37  
38  
39  
40  
41 **Figure 6.** Standard curve of glucose at pH 7.5 using compound **13**. The concentration of  
42 compound **13** was 10 nM. Chemiluminescence was measured for 1 min.  
43  
44  
45  
46  
47

48 **Theoretical Analysis.** The potential energy of the  $S_0$  state for compound **1** has been  
49 theoretically explored in detail by Błażejowski *et al.*<sup>56,60</sup>; the energy diagrams on the electronic  
50 ground state ( $S_0$ ) has been determined for 10-methyl-9-(phenoxy-carbonyl)acridium cations  
51 substituted with various alkyl groups in the phenyl fragment. However, the final products were  
52  
53  
54  
55  
56  
57  
58  
59  
60

1  
2  
3 assumed to be the electronic ground states for *N*-methylacridone (NMA) in their work. To make  
4  
5 acridone molecule emit a photon, the electronically excited states of NMA have to be found at  
6  
7 the end of this reaction in the proposed CL reaction mechanism by McCapra and Nelson.<sup>45,46a</sup> In  
8  
9 the present work, the energetics was mainly explored by density functional theory (DFT) based  
10  
11 B3-LYP functional at the correlation-consistent polarized-valence double-zeta (cc-pVDZ) basis  
12  
13 function<sup>61</sup> for (i) the thermally accessible dioxetanone to reach an electronic excited state of  
14  
15 acridone molecule in  $S_0$ , (ii) nonadiabatic transition through spin-orbit coupling between  $S_0$  and  
16  
17  $T_1$ , and (iii) the final decomposition to reach acridone in  $T_1$ . The first triplet state ( $T_1$ ) is  
18  
19 electronically excited state from the viewpoint of singlet calculations based on the DFT approach,  
20  
21 but since our interest is in the electronically ground state in triplet states, the DFT approach for  
22  
23 the triplet ground state ( $T_1$ ) was assumed to be reasonable for searching the reaction-path, rather  
24  
25 than TDFT approach. Polarized continuum model was also employed to reproduce the solvent  
26  
27 effect caused by dimethyl sulfoxide (DMSO). Each energy listed in Figure 7 was confirmed by a  
28  
29 single-point calculation at symmetry adapted cluster / configuration interaction (SAC-CI)  
30  
31 method with using the optimized geometry by the DFT calculation employing the same PCM by  
32  
33 DMSO (Table S2 in supporting information).

34  
35  
36 Since the mechanism of the nucleophilic addition of hydroperoxide anion was proposed by  
37  
38 McCapra and Nelson *et al.*<sup>45,46a</sup> and theoretically discussed by Błażejowski *et al.*,<sup>56,60</sup> the charges  
39  
40 of acridinium ester were evaluated by natural bond orbital (NBO) analysis. The atomic charge of  
41  
42 N10 position of compound **1** shows the negative charge which is about -0.343 (-0.303) at B3-  
43  
44 LYP (M06-2X); the hydroperoxide anion could be repulsive to N10 side.  
45  
46  
47  
48  
49  
50  
51  
52  
53  
54  
55  
56  
57  
58  
59  
60



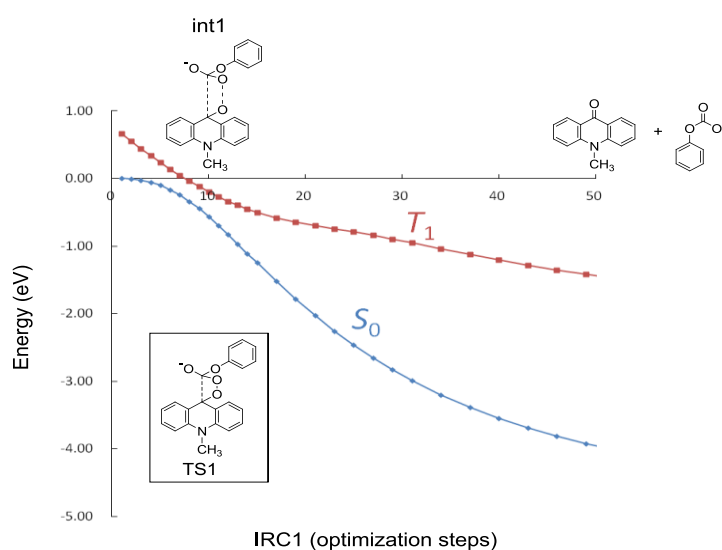
**Figure 7.** The energy diagram on the chemiluminescence mechanism proposed by McCapra and Nelson *et al.*<sup>45,46a</sup> (A) compound **1** (B) compound **3**.

Figure 7A shows the energy diagram started from the dioxetanone ring-structure (**min1**) for compound **1**, which was a stable dioxetane intermediate found by Błażejowski *et al.*<sup>56,60</sup> and then the transition state (TS) search was performed with the initial coordinate given by this **min1** structure, because the driving force for this reaction would assumed to be thermal decomposition.

1  
2  
3 The TS structure appeared at **TS1** to be close to the dioxetane intermediate (**min1**) as was  
4 expected; the C-C bond distance in the dioxetane structure was slightly stretched, compared with  
5  
6 **min1**. And then the reaction path (**IRC1**) on the electronic ground state ( $S_0$ ) was obtained from  
7  
8 the intrinsic reaction coordinate (IRC) analysis with the TS structure (**TS1**). The reaction path  
9  
10 (**IRC1**) determined by the IRC-analysis from **TS1** was found to be correlated to the interaction  
11  
12 structure between the  $S_0$  and lowest triplet ( $T_1$ ) states at **int1** (Figure 8), which clearly shows the  
13  
14 triplet state lying closely to  $S_0$ . Furthermore, the  $S_1$  state was much higher than  $T_1$  at **int1** (Table  
15  
16 S2(a) in supporting information); the vertical excitation energy of  $S_1$  was 2.02 eV at the  $S_0-T_1$   
17  
18 closest point (**int1**) by SAC-CI calculation.  
19  
20  
21  
22  
23

24  
25 As discussed in Ref. 62, the inter-system crossing (ISC, nonadiabatic transition in other  
26  
27 words) mechanism was explored due to the spin-orbit coupling between  $S_0$  and  $T_1$  states along  
28  
29 the reaction path of **IRC1**. The potential energy curve of the  $T_1$  state was found to be lying  
30  
31 closely to  $S_0$  at **int1**. Thus, the nonadiabatic transition between  $S_0$  and  $T_1$  could happen due to the  
32  
33 spin-orbit coupling effect at the vicinity to  $T_1$ .<sup>63</sup> If we here assumed the nonadiabatic transition  
34  
35 between  $S_0$  and  $T_1$ , the molecule could be expected to hop to  $T_1$  and be dissociated into 10-  
36  
37 methyl-9-acridone and the fragment anion in  $T_1$ ; it follows that the IRC-analysis was performed  
38  
39 again on  $T_1$  with the **int1** structure instead of **IRC1**. The obtained reaction path (**IRC2**) is found  
40  
41 to be correlated with the decomposition product including the triplet state of 10-methyl-9-  
42  
43 acridone, compared to **IRC1**; the phosphorescence could be anticipated by this process.  
44  
45 Furthermore, the transition probability due to the spin-orbit coupling was estimated by Zhu-  
46  
47 Nakamura formula;<sup>63</sup> the spin-orbit coupling elements were computed by complete active space  
48  
49 (CAS) SCF calculation by *ab initio* program package Molpro 2012 at cc-pVDZ basis set.<sup>64</sup>  
50  
51  
52  
53 Using 8 cpu-cores of AMD Opteron 2382 and 8 GB ram (Tempest9D2 model, CONCURRENT  
54  
55  
56  
57  
58  
59  
60

SYSTEM ltd.) in Sophia University, it took about four months to obtain all results. However, spin-orbit coupling elements were obtained by complete active space (CAS) SCF methods at cc-pVDZ basis set. The active space was determined by (6e, 4o); the electron configurations of CASSCF were totally 32,758. The probability was 96% at the **int1** structure by the available excess-energy proposed by Błażejowski *et al.*<sup>56,60</sup> In general, the transition probability is considered to be small for singlet–triplet transition, but there are several evidences discussed on nonadiabatic transition probability between singlet and triplet states;<sup>65</sup> the probabilities shown in several molecular systems are actually almost unity for intersystem crossing (ISC).



**Figure 8.** The intrinsic reaction coordinate determined with the initial molecular geometry of TS1 (IRC1). The employed step-width was 0.05 Bohr around TS.

Finally, the phosphorescence might happen, because the 10-methyl-9-acridone staying in  $T_1$  could emit photon for deactivating the excited 10-methyl-9-acridone. The phosphorescence process is discussed in the later paragraph.

1  
2  
3 We also carried out the same theoretical analysis on the compound **3** as shown in Figure 7B;  
4 the height of TS from **min2** to **TS2** was 0.05 eV, which was much smaller than the case of the  
5 compound **1** (0.76 eV). The 4-cyanophenol moiety in compound **3**, moreover, leaved along  
6 **IRC3** and the stable dioxetanone was produced at **min3**. The potential energy of  $S_0$  was found to  
7 be lying closely to the triplet state ( $T_1$ ) at this **min3**. Since the  $S_1$  state was much higher than  $T_1$   
8 (see Table S2(b)), the transition by ISC to the triplet state could be crucial on the CL of  
9 compound **3**.  
10  
11

12  
13  
14  
15  
16  
17  
18  
19  
20 The potential energy of the  $S_0$  state for compound **1** has been theoretically explored by  
21 Błażejowski,<sup>56,60</sup> but the exploration of electronically excited states is still necessary for the  
22 photoemission process of 10-methyl-9-acridone at the end of this reaction. It's because the  
23 electronically excited state ( $S_1$  or  $T_1$ ) of 10-methyl-9-acridone should appear as the thermal  
24 reaction product through  $S_0$ ; there should be two possible paths by nonadiabatic transition to  $S_1$   
25 or  $T_1$ . If we are considering that the nonadiabatic transition of  $S_0 - S_1$  will happen, the energy  
26 separation ( $\Delta E$ ) between these states should be less than 1.0 eV. Figure 7 and Table S2 however  
27 suggest that this  $S_0 - S_1$  transition would not occur because of  $\Delta E > 2.0$  eV. On the other hand, if  
28 the nonadiabatic transition of  $S_0 - T_1$  will happen, it would happen because of  $\Delta E < 1.0$  eV and  
29 our estimated probability by 96% at the **int1** structure, but phosphorescence process should be  
30 explored at the end of the reaction. The acridinium 4-cyanophenyl ester of compound **3** should  
31 be also explored in the same manner, because the reaction path on  $S_0$  was found to be quite  
32 different from compound **1** as shown in Figure 7. As clearly seen in Table S2, the  $S_1$  state is  
33 much higher than  $T_1$  at each molecular conformation except at products (i.e. 10-methyl-9-  
34 acridone). Although we were not able to perform the molecular geometry-optimization and IRC-  
35 calculation on each conformation at SAC-CI level, the obtained triplet states reasonably agree  
36  
37  
38  
39  
40  
41  
42  
43  
44  
45  
46  
47  
48  
49  
50  
51  
52  
53  
54  
55  
56  
57  
58  
59  
60

1  
2  
3 with the trend of DFT results, especially at the geometry of the  $S_0 - T_1$  closest point at **int1** and  
4  
5 **min3**. Here we are assuming the photoemission from the  $T_1$  state lying closely to the  $S_1$  state  
6  
7 (4.15 eV at SAC-CI) at the equilibrium geometry of 10-methyl-9-acridone, the expected  
8  
9 emission energy would be 2.43 eV at DFT (3.88 eV at SAC-CI). This emission energy from  $T_1$   
10  
11 quite agrees with the experimental spectrum which features the maximum speak at 430 nm (2.88  
12  
13 eV). However, since the transition dipole moment between  $S_1$  and  $S_0$  is 1.25  $a_0$  at the equilibrium  
14  
15 conformation of 10-methyl-9-acridone, the acridone would produce luminescence on the way of  
16  
17 the final dissociation processes in **IRC2** and **IRC4**, together with vibronic allowed transitions  
18  
19 described by the intensity borrowing mechanism (due to spin-orbit mixing) between these two  
20  
21 excited states ( $S_1$  and  $T_1$ ) lying closely to each other. The photoemission would happen in the  
22  
23 middle of these decomposition processes.  
24  
25  
26  
27  
28

29 On the other hand, the direct search for the minimum energy conical intersection (MECI)  
30  
31 between  $S_0$  and  $T_1$  for both compounds **1** and **3** were performed to make sure of our discussion;  
32  
33 we carried out the state-averaged CAS(6e,4o)SCF optimizations of a singlet-triplet conical  
34  
35 intersection in vacuo.<sup>64</sup> The result is shown in Figure S6 (supporting information) for compound  
36  
37 **1**, which is similar to the **int1** structure shown in Figure 7A. Concerning compound **3**, we also  
38  
39 found the MECI structure at around the **min3** structure shown in Figure 7B. Thus, the thermal  
40  
41 decomposition of acridanyl dioxetanes would happen along our proposal. It is furthermore found  
42  
43 that the solvent effect (DMSO) could not cause the different paths in compounds **1** and **3**, albeit  
44  
45 indirectly. As a result of these factors and the energy difference between **TS1** and **TS2** (barrier-  
46  
47 height,  $\Delta E=0.76$  and 0.05 eV), we could conclude that the *p*-cyanophenolate anion is more  
48  
49 stabilized than the phenolate anion in thermal decomposition processes, which leads to the  
50  
51  
52  
53  
54  
55  
56  
57  
58  
59  
60

1  
2  
3 difference between the paths for compounds **1** and **3**. Compound **3** could show the stronger  
4  
5 fluorescence intensity than compound **1**.  
6  
7

8  
9 Furthermore, the spin-orbit coupling was also evaluated at this CASSCF level with the MECI  
10 structure for compound **1**. The potential energies of  $S_0$  and  $T_1$  states were shifted due to the spin-  
11 orbit coupling, as shown in Table S3 (supporting information); the shifted energy range is  
12 approximately  $80 \text{ cm}^{-1}$ . Since the value of atomic carbon is  $43.4 \text{ cm}^{-1}$ ,<sup>66</sup> this shifted range is  
13 obviously larger than the normal carbon atom. Probably the carbon atoms are strongly affected  
14 by the oxygen atoms. Thus, our result could reasonably support the reaction pathway through  
15 the triplet state ( $T_1$ ).  
16  
17  
18  
19  
20  
21  
22  
23  
24  
25  
26  
27

## 28 CONCLUSION

29  
30  
31  
32 Various acridinium ester derivatives were synthesized and the chemiluminescence intensities  
33 were cleared. Acridinium esters that show strong chemiluminescence intensities under neutral  
34 conditions were identified. The introduction of electron-withdrawing groups at the 4-position of  
35 the phenyl and biphenyl moiety was very effective for increasing chemiluminescence intensity;  
36 the effect would induce the polarizability not only at the specific positions in acridine moiety, but  
37 also the strong polarizability as a whole molecule. 3,4-(Dimethoxycarbonyl)phenyl 10-methyl-  
38  $10\lambda^4$ -acridine-9-carboxylate, trifluoromethanesulfonate salt was useful compound for the  
39 determination of hydrogen peroxide and glucose under neutral conditions. The  
40 chemiluminescence reaction mechanism has been proposed by McCapra and Nelson, *et al.*<sup>45,46a</sup>  
41  
42 The proposed mechanism was mainly evaluated via quantum chemical calculation on density  
43 functional theory with the polarizable continuum model. The actual proposed mechanism was  
44  
45  
46  
47  
48  
49  
50  
51  
52  
53  
54  
55  
56  
57  
58  
59  
60

1  
2  
3 composed of the nucleophilic addition reaction of hydroperoxide anion, the highly strained  
4 dioxetanone ring formation and the decomposition of the ring molecule. Natural bond orbital  
5 (NBO) charge analysis shows that the atomic charge of C9 position in acridine moiety was  
6 obviously positive than the other atoms, and was quite attractive to a nucleophilic reagent such as  
7 hydroperoxide anion. The decomposition reaction would happen after the formation of the  
8 dioxetane intermediate; there was a transition state (TS) on the way of this decomposition, and it  
9 would be a rate-determining step in the whole process. Since the first triplet state ( $T_1$ ) was lying  
10 closely to  $S_0$  at around TS, nonadiabatic transition of  $S_0 \rightarrow T_1$  could happen, but the photoemission  
11 of the mixed state from  $T_1$  and  $S_1$  states of 10-methyl-9-acridone was expected due to the  
12 intensity borrowing mechanism at the end of the reaction. This mechanism would be consistent  
13 with the experimental result. This study should provide significant information toward the  
14 development of novel chemiluminescent acridinium esters.  
15  
16  
17  
18  
19  
20  
21  
22  
23  
24  
25  
26  
27  
28  
29  
30  
31  
32  
33

## 34 EXPERIMENTAL SECTION

35  
36  
37  
38 **General Information.** Melting points were uncorrected.  $^1\text{H}$  and  $^{13}\text{C}$  NMR spectra were  
39 recorded on a 500 MHz and 125.7 MHz spectrometers. HRMS spectra were obtained by  
40 electrospray ionization time-of-flight (ESI-TOF) system or fast atom bombardment (FAB).  
41  
42  
43  
44

45  
46 **General Procedure for the Synthesis of Compounds 1–17.** To a solution of acridine-9-  
47 carbonyl chloride (0.12 g, 0.5 mmol) in dry tetrahydrofuran (10 mL) under nitrogen gas was  
48 added 4-dimethylaminopyridine (0.01 g, 0.08 mmol), the corresponding phenols (0.75 mmol)  
49 and triethylamine (2 mL). The mixture was refluxed for 2.5 h. Chloroform (150 mL) and water  
50 (100 mL) were added to the solution. The organic layer was dried with anhydrous sodium  
51  
52  
53  
54  
55  
56  
57  
58  
59  
60

1  
2  
3 sulfate. The filtrate was evaporated in vacuo, and the residue was purified by column  
4 chromatography (silica gel, chloroform or ethyl acetate-hexane solution) to produce the desired  
5 acridine-9-carboxylates. The acridine-9-carboxylates were *N*-methylated by methyl  
6 trifluoromethanesulfonate in dichloromethane, which were purified by column chromatography  
7 (silica gel, chloroform-methanol) to produce the desired acridine-9-carboxylates,  
8 trifluoromethanesulfonate salt.  
9  
10

11  
12  
13 **Phenyl 10-methyl-10 $\lambda^4$ -acridine-9-carboxylate, trifluoromethanesulfonate salt (1).** Yellow  
14 solid (0.01 g, 13%); mp 233–235 °C; <sup>1</sup>H NMR (500 MHz, Acetone-*d*<sub>6</sub>):  $\delta$  5.25 (s, 3H), 7.48 (m,  
15 1H), 7.63 (m, 2H), 7.69 (m, 2H), 8.26 (m, 2H), 8.64 (m, 2H), 8.75 (d, *J* = 8.5 Hz, 2H), 9.06 (d, *J*  
16 = 9.5 Hz, 2H); <sup>13</sup>C NMR (125.7 MHz, DMSO-*d*<sub>6</sub>):  $\delta$  119.9, 121.8, 122.2, 127.5, 129.8, 130.1,  
17 139.1, 141.9, 146.8, 149.5, 163.5; HRMS ESI (*m/z*) calculated for C<sub>21</sub>H<sub>16</sub>NO<sub>2</sub> [M]<sup>+</sup> 314.1181,  
18 found 314.1177.  
19  
20

21  
22  
23 ***p*-Tolyl 10-methyl-10 $\lambda^4$ -acridine-9-carboxylate, trifluoromethanesulfonate salt (2).** Yellow  
24 solid (0.03 g, 14%); mp 232–234 °C; <sup>1</sup>H NMR (500 MHz, Acetone-*d*<sub>6</sub>):  $\delta$  2.43 (s, 3H), 5.24 (s,  
25 3H), 7.43 (d, *J* = 8 Hz, 2H), 7.55 (d, *J* = 8.5 Hz, 2H), 8.25 (m, 2H), 8.64 (m, 2H), 8.72 (d, *J* = 8.5  
26 Hz, 2H), 9.05 (d, *J* = 9.5 Hz, 2H); <sup>13</sup>C NMR (125.7 MHz, DMSO-*d*<sub>6</sub>)  $\delta$  20.4, 119.9, 121.5, 122.2,  
27 127.5, 129.7, 130.4, 136.9, 139.1, 141.9, 146.9, 147.3, 163.6; HRMS ESI (*m/z*) calculated for  
28 C<sub>22</sub>H<sub>18</sub>NO<sub>2</sub> [M]<sup>+</sup> 328.1338, found 328.1361.  
29  
30

31  
32  
33 **4-Cyanophenyl 10-methyl-10 $\lambda^4$ -acridine-9-carboxylate, trifluoromethanesulfonate salt**  
34 **(3).** Yellow solid (0.05 g, 23%); mp 278–280 °C; <sup>1</sup>H NMR (500 MHz, Acetone-*d*<sub>6</sub>):  $\delta$  5.25 (s,  
35 3H), 7.98 (d, *J* = 8.5 Hz, 2H), 8.08 (d, *J* = 8.5 Hz, 2H), 8.25 (m, 2H), 8.64 (m, 2H), 8.78 (d, *J* =  
36 8.5 Hz, 2H), 9.07 (d, *J* = 9 Hz, 2H); <sup>13</sup>C NMR (125.7 MHz, DMSO-*d*<sub>6</sub>):  $\delta$  110.6, 118, 119.9,  
37 127.5, 129.7, 130.4, 136.9, 139.1, 141.9, 146.9, 147.3, 163.6; HRMS ESI (*m/z*) calculated for  
38 C<sub>22</sub>H<sub>18</sub>NO<sub>2</sub> [M]<sup>+</sup> 328.1338, found 328.1361.  
39  
40  
41  
42  
43  
44  
45  
46  
47  
48  
49  
50  
51  
52  
53  
54  
55  
56  
57  
58  
59  
60

1  
2  
3 122.3, 123.5, 127.5, 129.8, 134.6, 139.2, 141.9, 145.9, 152.5, 162.8; HRMS ESI (m/z) calculated  
4 for C<sub>22</sub>H<sub>15</sub>N<sub>2</sub>O<sub>2</sub> [M]<sup>+</sup> 339.1134; found 339.1139.  
5  
6

7  
8 **4-(Trifluoromethyl)phenyl 10-methyl-10λ<sup>4</sup>-acridine-9-carboxylate, trifluoromethane-**  
9 **sulfonate salt (4).** Yellow solid (0.03 g, 13%); mp 252–255 °C; <sup>1</sup>H NMR (500 MHz, Acetone-  
10 d<sub>6</sub>): δ 5.26 (s, 3H), 7.98 (m, 4H), 8.26 (m, 2H), 8.65 (m, 2H), 8.79 (d, *J* = 8.5 Hz, 2H), 9.07 (d, *J*  
11 = 9.5 Hz, 2H); <sup>13</sup>C NMR (125.7 MHz, DMSO-d<sub>6</sub>): δ 119.9, 121.9, 122.3, 122.7, 123.1, 124.9,  
12 127.1, 127.5, 128, 128.3, 129.2, 129.8, 139.2, 141.9, 146.1, 152.2, 163; HRMS ESI (m/z)  
13 calculated for C<sub>22</sub>H<sub>15</sub>F<sub>3</sub>NO<sub>2</sub> [M]<sup>+</sup> 382.1055; found 382.1055.  
14  
15  
16  
17  
18  
19  
20  
21

22  
23 **4-Methoxyphenyl 10-methyl-10λ<sup>4</sup>-acridine-9-carboxylate, trifluoromethanesulfonate salt**  
24 **(5).** Yellow solid (0.04 g, 25%); mp 265–268 °C; <sup>1</sup>H NMR (500 MHz, Acetone-d<sub>6</sub>) δ 3.88 (s,  
25 3H), 5.24 (s, 3H), 7.14 (d, *J* = 9 Hz, 2H), 7.6 (d, *J* = 9.5 Hz, 2H), 8.25 (m, 2H), 8.63 (m, 2H),  
26 8.71 (d, *J* = 8.5 Hz, 2H), 9.05 (d, *J* = 9 Hz, 2H); <sup>13</sup>C NMR (125.7 MHz, DMSO-d<sub>6</sub>) δ 55.7, 114.9,  
27 119.4, 119.8, 121.9, 122.2, 122.8, 127.5, 129.7, 139.1, 141.9, 142.8, 147, 158, 163.8; HRMS  
28 ESI (m/z) calculated for C<sub>22</sub>H<sub>18</sub>NO<sub>3</sub> [M]<sup>+</sup> 344.1287, found 344.1294.  
29  
30  
31  
32  
33  
34  
35  
36

37  
38 **4-Bromophenyl 10-methyl-10λ<sup>4</sup>-acridine-9-carboxylate, trifluoromethanesulfonate salt**  
39 **(6).** Yellow solid (0.11 g, 63%); mp 248–250 °C; <sup>1</sup>H NMR (500 MHz, Acetone-d<sub>6</sub>) δ 5.24 (s,  
40 3H), 7.7 (d, *J* = 9 Hz, 2H), 7.8 (d, *J* = 9 Hz, 2H), 8.24 (t, *J* = 8 Hz, 2H), 8.63 (m, 2H), 8.74 (d, *J*  
41 = 9 Hz, 2H), 9.05 (d, *J* = 9.5 Hz, 2H); <sup>13</sup>C NMR (125.7 MHz, DMSO-d<sub>6</sub>) δ 119.9, 120, 122.3,  
42 124.2, 127.5, 129.7, 132.9, 139.1, 141.9, 146.4, 148.6, 163.2; HRMS ESI (m/z) calculated for  
43 C<sub>21</sub>H<sub>15</sub>BrNO<sub>2</sub> [M]<sup>+</sup> 392.0286, found 392.0290.  
44  
45  
46  
47  
48  
49  
50  
51

52  
53 **4-Iodophenyl 10-methyl-10λ<sup>4</sup>-acridine-9-carboxylate, trifluoromethanesulfonate salt (7).**  
54 Yellow solid (0.05 g, 26%); mp 267–270 °C; <sup>1</sup>H NMR (500 MHz, Acetone-d<sub>6</sub>): δ 5.25 (s, 3H),  
55 7.56 (d, *J* = 9 Hz, 2H), 7.99 (d, *J* = 8.5 Hz, 2H), 8.24 (t, *J* = 7 Hz, 2H), 8.64 (m, 2H), 8.74 (d, *J* =  
56  
57  
58  
59  
60

1  
2  
3  
4  
5  
6  
7  
8  
9  
10  
11  
12  
13  
14  
15  
16  
17  
18  
19  
20  
21  
22  
23  
24  
25  
26  
27  
28  
29  
30  
31  
32  
33  
34  
35  
36  
37  
38  
39  
40  
41  
42  
43  
44  
45  
46  
47  
48  
49  
50  
51  
52  
53  
54  
55  
56  
57  
58  
59  
60

9 Hz, 2H), 9.05 (d,  $J = 9.5$  Hz, 2H);  $^{13}\text{C}$  NMR (125.7 MHz, DMSO- $d_6$ ):  $\delta$  92.7, 119.9, 122.3, 124.3, 127.5, 129.7, 138.8, 139.2, 141.9, 146.4, 149.3, 163.2; HRMS ESI ( $m/z$ ) calculated for  $\text{C}_{21}\text{H}_{15}\text{INO}_2$   $[\text{M}]^+$  440.0147; found 440.0140.

**4-Formylphenyl 10-methyl-10 $\lambda^4$ -acridine-9-carboxylate, trifluoromethanesulfonate salt (8).** Yellow solid (0.14 g, 57%); mp 255–258 °C;  $^1\text{H}$  NMR (500 MHz, Acetone- $d_6$ ):  $\delta$  5.26 (s, 3H), 7.96 (d,  $J = 8.5$  Hz, 2H), 8.2 (d,  $J = 6.5$  Hz, 2H), 8.26 (m, 2H), 8.65 (m, 2H), 8.79 (d,  $J = 9$  Hz, 2H), 9.07 (d,  $J = 9.5$  Hz, 2H), 10.15 (s, 1H);  $^{13}\text{C}$  NMR (125.7 MHz, DMSO- $d_6$ ):  $\delta$  119.9, 122.3, 122.9, 127.5, 129.8, 131.4, 135.2, 139.2, 141.9, 146.1, 153.6, 163, 192.1; HRMS ESI ( $m/z$ ) calculated for  $\text{C}_{22}\text{H}_{16}\text{NO}_3$   $[\text{M}]^+$  342.1130; found 342.1126.

**4-(Methoxycarbonyl)phenyl 10-methyl-10 $\lambda^4$ -acridine-9-carboxylate, trifluoromethanesulfonate salt (9).** Yellow solid (0.07 g, 30%); mp 250–253 °C;  $^1\text{H}$  NMR (500 MHz, Acetone- $d_6$ ):  $\delta$  3.96 (s, 3H), 5.25 (s, 3H), 7.88 (d,  $J = 8.5$  Hz, 2H), 8.25 (m, 4H), 8.65 (m, 2H), 8.77 (d,  $J = 9$  Hz, 2H), 9.07 (d,  $J = 9.5$  Hz, 2H);  $^{13}\text{C}$  NMR (125.7 MHz, DMSO- $d_6$ ):  $\delta$  52.4, 119.9, 122.3, 122.4, 127.5, 128.8, 129.8, 131.2, 139.2, 141.9, 146.2, 152.9, 163, 165.3; HRMS ESI ( $m/z$ ) calculated for  $\text{C}_{23}\text{H}_{18}\text{NO}_4$   $[\text{M}]^+$  372.1236; found 372.1222.

**4-(Ethoxycarbonyl)phenyl 10-methyl-10 $\lambda^4$ -acridine-9-carboxylate, trifluoromethanesulfonate salt (10).** Yellow solid (0.01 g, 4%); mp 258–260 °C;  $^1\text{H}$  NMR (500 MHz, Acetone- $d_6$ ):  $\delta$  1.38 (t,  $J = 7$  Hz, 3H), 4.39 (q,  $J = 7$  Hz, 2H), 5.26 (s, 3H), 7.86 (d,  $J = 9$  Hz, 2H), 8.25 (m, 4H), 8.65 (t,  $J = 8$  Hz, 2H), 8.77 (d,  $J = 8.5$  Hz, 2H), 9.07 (d,  $J = 10$  Hz, 2H);  $^{13}\text{C}$  NMR (125.7 MHz, DMSO- $d_6$ ):  $\delta$  14.1, 61.1, 119.9, 122.3, 122.4, 127.5, 129.1, 129.8, 131.1, 139.2, 141.9, 146.2, 152.8, 163, 164.8; HRMS ESI ( $m/z$ ) calculated for  $\text{C}_{24}\text{H}_{20}\text{NO}_4$   $[\text{M}]^+$  386.1392; found 386.1392.

**4-Nitrophenyl 10-methyl-10 $\lambda^4$ -acridine-9-carboxylate, trifluoromethanesulfonate salt (11).**

Yellow solid (0.07 g, 46%); mp 232–235 °C;  $^1\text{H}$  NMR (500 MHz, Acetone- $d_6$ ):  $\delta$  5.26 (s, 3H), 8.05 (d,  $J = 9$  Hz, 2H), 8.26 (m, 2H), 8.5 (d,  $J = 9$  Hz, 2H), 8.65 (m, 2H), 8.8 (d,  $J = 9$  Hz, 2H), 9.07 (d,  $J = 9.5$  Hz, 2H);  $^{13}\text{C}$  NMR (125.7 MHz, DMSO- $d_6$ )  $\delta$  119.9, 122.3, 123.5, 125.7, 127.5, 129.8, 139.2, 141.9, 145.8, 146.3, 153.8, 162.7. HRMS ESI ( $m/z$ ) calculated for  $\text{C}_{21}\text{H}_{15}\text{N}_2\text{O}_4$   $[\text{M}]^+$  359.1032, found 359.1052.

**3,4-Dicyanophenyl 10-methyl-10 $\lambda^4$ -acridine-9-carboxylate, trifluoromethanesulfonate salt (12).** Ocherous solid (0.03 g, 12%); mp 252–254 °C;  $^1\text{H}$  NMR (500 MHz, Acetone- $d_6$ ):  $\delta$  5.26 (s, 3H), 8.24 (m, 2H), 8.38 (s, 2H), 8.57 (t,  $J = 1.5$  Hz, 1H), 8.65 (m, 2H), 8.84 (d,  $J = 8$  Hz, 2H), 9.07 (d,  $J = 9.5$  Hz, 2H);  $^{13}\text{C}$  NMR (125.7 MHz, DMSO- $d_6$ ):  $\delta$  113, 113.9, 115, 115.3, 116.7, 119.8, 122.4, 127, 127.7, 128.1, 128.3, 129.3, 129.7, 136.2, 139.2, 141.9, 145.2, 152, 162.4; HRMS FAB ( $m/z$ ) calculated for  $\text{C}_{23}\text{H}_{14}\text{N}_3\text{O}_2$   $[\text{M}]^+$  364.1086; found 364.1090.

**3,4-(Dimethoxycarbonyl)phenyl 10-methyl-10 $\lambda^4$ -acridine-9-carboxylate, trifluoromethanesulfonate salt (13).** Yellow solid (0.03 g, 13%); mp 268–271 °C;  $^1\text{H}$  NMR (500 MHz, Acetone- $d_6$ ):  $\delta$  3.93 (s, 6H), 5.27 (s, 3H), 8.04 (m, 3H), 8.25 (m, 2H), 8.66 (m, 2H), 8.83 (d,  $J = 8.5$  Hz, 2H), 9.08 (d,  $J = 9.5$  Hz, 2H);  $^{13}\text{C}$  NMR (125.7 MHz, DMSO- $d_6$ ):  $\delta$  52.9, 113, 119.8, 122.3, 125, 126.9, 127.7, 129.6, 129.8, 134.2, 139.2, 141.9, 145.9, 151.2, 162.9, 166.1, 166.5; HRMS FAB ( $m/z$ ) calculated for  $\text{C}_{25}\text{H}_{20}\text{NO}_6$   $[\text{M}]^+$  430.1291; found 430.1274.

**[1,1'-Biphenyl]-4-yl 10-methyl-10 $\lambda^4$ -acridine-9-carboxylate, trifluoromethanesulfonate salt (14).** Yellow solid (0.06 g, 23%); mp 250–253 °C;  $^1\text{H}$  NMR (500 MHz, DMSO- $d_6$ ):  $\delta$  4.96 (s, 3H), 7.42 (t,  $J = 7$  Hz, 1H), 7.51 (t,  $J = 8$  Hz, 2H), 7.76 (d,  $J = 7.5$  Hz, 2H), 7.85 (d,  $J = 9$  Hz, 2H), 7.91 (d,  $J = 9$  Hz, 2H), 8.18 (t,  $J = 7$  Hz, 2H), 8.55 (t,  $J = 8$  Hz, 2H), 8.66 (d,  $J = 8.5$  Hz, 2H), 8.94 (d,  $J = 9$  Hz, 2H);  $^{13}\text{C}$  NMR (125.7 MHz, DMSO- $d_6$ ):  $\delta$  119.9, 122.3, 126.9, 127.5,

1  
2  
3 127.8, 128.3, 129, 129.8, 139, 139.2, 139.5, 141.9, 146.7, 148.9, 163.5; HRMS ESI (m/z)  
4  
5 calculated for  $C_{27}H_{20}NO_2$   $[M]^+$  390.1494; found 390.1514.  
6  
7

8 **Naphthalen-1-yl 10-methyl-10 $\lambda^4$ -acridine-9-carboxylate, trifluoromethanesulfonate salt**  
9  
10 **(15).** Yellow solid (0.04 g, 50%); mp 245–248 °C;  $^1H$  NMR (500 MHz, Acetone- $d_6$ ):  $\delta$  5.29 (s,  
11 3H), 7.62 (m, 2H), 7.74 (t,  $J = 8$  Hz, 1H), 8.01 (d,  $J = 8.5$  Hz, 1H), 8.06 (d,  $J = 8.5$  Hz, 1H), 8.11  
12 (d,  $J = 8$  Hz, 2H), 8.31(m, 2H), 8.68 (m, 2H), 8.84 (d,  $J = 8$  Hz, 2H), 9.1 (d,  $J = 9.5$  Hz, 2H);  $^{13}C$   
13 NMR (125.7 MHz, DMSO- $d_6$ ):  $\delta$  118.9, 120, 122.4, 125.4, 125.7, 127.1, 127.2, 127.3, 127.6,  
14 128.3, 129.9, 134.3, 139.2, 141.9, 144.9, 146.6, 163.4; HRMS ESI (m/z) calculated for  
15  $C_{25}H_{18}NO_2$   $[M]^+$  364.1338; found 364.1342.  
16  
17  
18  
19  
20  
21  
22  
23

24 **2-Oxo-2H-chromen-4-yl 10-methyl-10 $\lambda^4$ -acridine-9-carboxylate, trifluoromethane-**  
25 **sulfonate salt (16).** Yellow solid (0.01 g, 4%); mp 238–241 °C;  $^1H$  NMR (500 MHz, Acetone-  
26  $d_6$ ):  $\delta$  3.63 (s, 3H), 6.29 (s, 1H), 6.78 (m, 1H), 7.1 (m, 3H), 7.28 (d,  $J = 8.5$  Hz, 1H), 7.33 (d,  $J =$   
27 9 Hz, 2H), 7.48 (m, 2H), 7.56 (m, 1H), 7.6 (m, 2H);  $^{13}C$  NMR (125.7 MHz, DMSO- $d_6$ ):  $\delta$  91,  
28 115.7, 116.3, 117.3, 119.6, 120.7, 121.5, 123.2, 123.9, 128, 128.9, 132.7, 138.9, 140.8, 141.8,  
29 151.3, 153.5, 161.8, 165.6, 166.3; HRMS ESI (m/z) calculated for  $C_{24}H_{16}NO_4$   $[M]^+$  382.1079;  
30 found 382.1088.  
31  
32  
33  
34  
35  
36  
37  
38  
39  
40  
41

42 **(3-Oxo-1,3-dihydroisobenzofuran-1,1-diyl)bis(4,1-phenylene) bis(10-methyl-10 $\lambda^4$ -**  
43 **acridine-9-carboxylate), ditrifluoromethanesulfonate salt (17).** Yellow solid (0.13 g, 21%);  
44 mp 280–283 °C;  $^1H$  NMR (500 MHz, DMSO- $d_6$ ):  $\delta$  4.95 (s, 6H), 7.60 (d,  $J = 9$  Hz, 1H), 7.66  
45 (m, 3H), 7.73 (d,  $J = 9$  Hz, 1H), 7.77 (m, 2H), 7.84 (m, 3H), 7.96 (m, 2H), 8.03 (m, 1H), 8.13 (m,  
46 4H), 8.26 (d,  $J = 9$  Hz, 1H), 8.29 (d,  $J = 9$  Hz, 1H), 8.53 (m, 3H), 8.61 (d,  $J = 8.5$  Hz, 3H), 8.93  
47 (d,  $J = 9.5$  Hz, 3H);  $^{13}C$  NMR (125.7 MHz, DMSO- $d_6$ ):  $\delta$  89.9, 119.4, 119.9, 121.4, 122, 122.3,  
48 122.4, 122.5, 124.3, 124.7, 124.8, 126, 127.4, 128.4, 128.5, 129.1, 129.8, 130.5, 131.5, 135.5,  
49  
50  
51  
52  
53  
54  
55  
56  
57  
58  
59  
60

1  
2  
3 139.1, 139.2, 139.7, 139.8, 142, 146.4, 147.5, 149.6, 149.7, 150.1, 150.8, 150.9, 163.3, 165.2,  
4  
5 168.5, 168.6; HRMS ESI (m/z) calculated for C<sub>50</sub>H<sub>34</sub>N<sub>2</sub>O<sub>6</sub> [M]<sup>2+</sup> 379.1209; found 379.1220.  
6  
7

8 **General Procedure for the Synthesis of Compounds 18–26.** To a solution of acridine-9-  
9 carbonyl chloride (0.12 g, 0.5 mmol) in dry tetrahydrofuran (10 mL) under nitrogen gas was  
10 added 4-dimethylaminopyridine (0.03 g, 0.25 mmol), the corresponding biphenols (0.75 mmol)  
11 and triethylamine (1.5 mL). The mixture was refluxed for 2.5 h. Chloroform (150 mL) and  
12 water (100 mL) were added to the solution. The organic layer was dried with anhydrous sodium  
13 sulfate. The filtrate was concentrated and purified by column chromatography (silica gel,  
14 chloroform) to produce the desired acridine-9-carboxylates. The acridine-9-carboxylates were  
15 *N*-methylated by methyl trifluoromethanesulfonate in dichloromethane, which were purified by  
16 column chromatography (silica gel, chloroform-methanol) to produce the desired acridine-9-  
17 carboxylates, trifluoromethanesulfonate salt.  
18  
19  
20  
21  
22  
23  
24  
25  
26  
27  
28  
29  
30

31  
32 **4'-Methyl-[1,1'-biphenyl]-4-yl 10-methyl-10λ<sup>4</sup>-acridine-9-carboxylate, trifluoromethane-**  
33 **sulfonate salt (18).** Yellow solid (0.1 g, 33%); mp 278–281 °C; <sup>1</sup>H NMR (500 MHz, DMSO-  
34 d<sub>6</sub>): δ 2.37 (s, 3H), 4.96 (s, 3H), 7.32 (d, *J* = 8 Hz, 2H), 7.61 (d, *J* = 8.5 Hz, 1H), 7.65 (d, *J* = 8  
35 Hz, 2H), 7.82 (m, 3H), 8.18 (m, 2H), 8.55 (m, 2H), 8.62 (m, 2H), 8.93 (m, 2H); <sup>13</sup>C NMR (125.7  
36 MHz, DMSO-d<sub>6</sub>): δ=20.6, 119.9, 122.3, 124.3, 126.7, 127.5, 128, 129.6, 129.8, 136.1, 137.2,  
37 138.8, 139.2, 139.4, 141.9, 146.4, 146.8, 148.7, 149.3, 163.2, 163.5; HRMS ESI (m/z)  
38 calculated for C<sub>28</sub>H<sub>22</sub>NO<sub>2</sub> [M]<sup>+</sup> 404.1651; found 404.1678.  
39  
40  
41  
42  
43  
44  
45  
46  
47  
48

49 **4'-Ethyl-[1,1'-biphenyl]-4-yl 10-methyl-10λ<sup>4</sup>-acridine-9-carboxylate, trifluoromethane-**  
50 **sulfonate salt (19).** Yellow solid (0.02 g, 5%); mp 265–268 °C; <sup>1</sup>H NMR (500 MHz, DMSO-  
51 d<sub>6</sub>): δ 1.22 (t, *J* = 7.5 Hz, 3H), 2.65 (q, *J* = 7.5 Hz, 2H), 4.96 (s, 3H), 7.35 (d, *J* = 8 Hz, 2H), 7.61  
52 (d, *J* = 8.5 Hz, 1H), 7.67 (d, *J* = 8.5 Hz, 2H), 7.82 (d, *J* = 9 Hz, 1H), 7.88 (d, *J* = 8.5 Hz, 1H),  
53  
54  
55  
56  
57  
58  
59  
60

7.99 (d,  $J = 8.5$  Hz, 1H), 8.15 (m, 2H), 8.53 (m, 2H), 8.62 (d,  $J = 8.5$  Hz, 1H), 8.66 (d,  $J = 9$  Hz, 1H), 8.93 (m, 2H);  $^{13}\text{C}$  NMR (125.7 MHz, DMSO- $d_6$ ):  $\delta = 15.5, 27.8, 119.9, 122.3, 124.3, 126.8, 127.5, 128, 128.4, 129.8, 136.4, 138.8, 139.2, 139.5, 141.9, 143.5, 146.4, 146.8, 148.7, 149.3, 163.2, 163.5$ ; HRMS FAB (m/z) calculated for  $\text{C}_{29}\text{H}_{24}\text{NO}_2$   $[\text{M}]^+$  418.1807; found 418.1813.

**4'-Methoxy-[1,1'-biphenyl]-4-yl 10-methyl-10 $\lambda^4$ -acridine-9-carboxylate, trifluoromethanesulfonate salt (20).** Yellow solid (0.05 g, 12%); mp 255–258 °C;  $^1\text{H}$  NMR (500 MHz, DMSO- $d_6$ ):  $\delta$  3.82 (s, 3H), 4.96 (s, 3H), 7.07 (d,  $J = 8.5$  Hz, 2H), 7.7 (d,  $J = 9$  Hz, 2H), 7.8 (d,  $J = 9$  Hz, 2H), 7.85 (d,  $J = 8.5$  Hz, 2H), 8.18 (t,  $J = 7$  Hz, 2H), 8.55 (t,  $J = 8$  Hz, 2H), 8.65 (d,  $J = 8.5$  Hz, 2H), 8.94 (d,  $J = 9.5$  Hz, 2H);  $^{13}\text{C}$  NMR (125.7 MHz, DMSO- $d_6$ ):  $\delta$  55.2, 112.9, 114.4, 119.9, 121.2, 122.2, 122.3, 127.2, 127.5, 127.7, 128, 129.8, 131.3, 139.2, 141.9, 146.8, 148.4, 159.2, 163.5; HRMS FAB (m/z) calculated for  $\text{C}_{28}\text{H}_{22}\text{NO}_3$   $[\text{M}]^+$  420.1600; found 420.1614.

**4'-Bromo-[1,1'-biphenyl]-4-yl 10-methyl-10 $\lambda^4$ -acridine-9-carboxylate, trifluoromethanesulfonate salt (21).** Yellow solid (0.08 g, 29%); mp 262–265 °C;  $^1\text{H}$  NMR (500 MHz, DMSO- $d_6$ ):  $\delta$  4.96 (s, 3H), 7.7 (m, 4H), 7.86 (d,  $J = 9$  Hz, 2H), 7.92 (d,  $J = 9$  Hz, 2H), 8.17 (t,  $J = 7$  Hz, 2H), 8.55 (t,  $J = 9.5$  Hz, 2H), 8.66 (d,  $J = 8.5$  Hz, 2H), 8.94 (d,  $J = 9.5$  Hz, 2H);  $^{13}\text{C}$  NMR (125.7 MHz, DMSO- $d_6$ ):  $\delta$  112.9, 119.9, 121.3, 121.4, 122.3, 122.4, 126.9, 127.5, 127.8, 128.3, 128.6, 129, 129.1, 129.8, 131.7, 131.9, 138.1, 138.2, 139.2, 141.9, 146.6, 149.2, 163.4; HRMS FAB (m/z) calculated for  $\text{C}_{27}\text{H}_{19}\text{BrNO}_2$   $[\text{M}]^+$  468.0599; found 468.0627.

**4'-(Methoxycarbonyl)-[1,1'-biphenyl]-4-yl 10-methyl-10 $\lambda^4$ -acridine-9-carboxylate, trifluoromethanesulfonate salt (22).** Yellow solid (0.09 g, 11%); mp 254–257 °C;  $^1\text{H}$  NMR (500 MHz, DMSO- $d_6$ ):  $\delta$  3.9 (s, 3H), 4.96 (s, 3H), 7.9 (d,  $J = 8.5$  Hz, 2H), 7.93 (d,  $J = 9$  Hz, 2H), 8 (d,  $J = 9$  Hz, 2H), 8.09 (d,  $J = 8.5$  Hz, 2H), 8.18 (t,  $J = 8$  Hz, 2H), 8.55 (t,  $J = 9.5$  Hz, 2H), 8.67 (d,  $J = 8$  Hz, 2H), 8.94 (d,  $J = 9.5$  Hz, 2H);  $^{13}\text{C}$  NMR (125.7 MHz, DMSO- $d_6$ ):  $\delta$  52.2, 119.9, 121.5,

1  
2  
3 122.3, 122.5, 126.8, 127.2, 127.5, 128.2, 128.7, 128.8, 129.8, 138.1, 139.2, 141.9, 143.4, 146.6,  
4  
5 149.6, 163.4, 166; HRMS FAB (m/z) calculated for C<sub>29</sub>H<sub>22</sub>NO<sub>4</sub> [M]<sup>+</sup> 448.1549; found 448.1524.  
6  
7

8 **4'-(Ethoxycarbonyl)-[1,1'-biphenyl]-4-yl 10-methyl-10λ<sup>4</sup>-acridine-9-carboxylate, tri-**  
9  
10 **fluoromethanesulfonate salt (23).** Yellow solid (0.12 g, 20%); mp 226–229 °C; <sup>1</sup>H NMR (500  
11  
12 MHz, DMSO-d<sub>6</sub>): δ 1.34 (t, *J* = 7 Hz, 3H), 4.34 (q, *J* = 7 Hz, 2H), 4.96 (s, 3H), 7.9 (d, *J* = 9 Hz,  
13  
14 2H), 7.92 (d, *J* = 8.5 Hz, 2H), 8 (d, *J* = 8.5 Hz, 2H), 8.08 (d, *J* = 8.5 Hz, 2H), 8.18 (t, *J* = 8.5 Hz,  
15  
16 2H), 8.55 (t, *J* = 9 Hz, 2H), 8.67 (d, *J* = 8.5 Hz, 2H), 8.94 (d, *J* = 9 Hz, 2H); <sup>13</sup>C NMR (125.7  
17  
18 MHz, DMSO-d<sub>6</sub>): δ 14.1, 60.8, 119.9, 122.3, 122.5, 127.1, 127.5, 128.7, 129.1, 129.8, 138.2,  
19  
20 139.2, 141.9, 143.3, 146.6, 149.6, 163.4, 165.5; HRMS FAB (m/z) calculated for C<sub>30</sub>H<sub>24</sub>NO<sub>4</sub>  
21  
22 [M]<sup>+</sup> 462.1705; found 462.1685.  
23  
24  
25  
26

27 **4'-((Benzyloxy)carbonyl)-[1,1'-biphenyl]-4-yl 10-methyl-10λ<sup>4</sup>-acridine-9-carboxylate, tri-**  
28  
29 **fluoromethanesulfonate salt (24).** Yellow solid (0.04 g, 9%); mp 222–225 °C. <sup>1</sup>H NMR (500  
30  
31 MHz, DMSO-d<sub>6</sub>): δ 4.96 (s, 3H), 5.4 (s, 2H), 7.37 (d, *J* = 7 Hz, 1H), 7.41 (t, *J* = 8 Hz, 2H), 7.49  
32  
33 (d, *J* = 7 Hz, 2H), 7.9 (d, *J* = 8.5 Hz, 2H), 7.93 (d, *J* = 8.5 Hz, 2H), 7.99 (d, *J* = 9 Hz, 2H), 8.12  
34  
35 (d, *J* = 8.5 Hz, 2H), 8.18 (m, 2H), 8.55 (t, *J* = 9 Hz, 2H), 8.67 (d, *J* = 8.5 Hz, 2H), 8.94 (d, *J* = 9  
36  
37 Hz, 2H); <sup>13</sup>C NMR (125.7 MHz, DMSO-d<sub>6</sub>): δ=66.2, 119.9, 122.3, 122.6, 127.3, 127.5, 127.9,  
38  
39 128.1, 128.5, 128.7, 128.8, 129.8, 129.9, 136.1, 138.1, 139.2, 141.9, 143.6, 146.6, 149.6, 163.4,  
40  
41 165.3; HRMS FAB (m/z) calculated for C<sub>35</sub>H<sub>26</sub>NO<sub>4</sub> [M]<sup>+</sup> 524.1862; found 524.1861.  
42  
43  
44  
45  
46

47 **4'-Nitro-[1,1'-biphenyl]-4-yl 10-methyl-10λ<sup>4</sup>-acridine-9-carboxylate, trifluoromethane-**  
48  
49 **sulfonate salt (25).** Yellow solid (0.13 g, 45%); mp > 300 °C; <sup>1</sup>H NMR (500 MHz, DMSO-d<sub>6</sub>):  
50  
51 δ 4.97 (s, 3H), 7.94 (d, *J* = 8.5 Hz, 2H), 8.05 (t, *J* = 8.5 Hz, 4H), 8.18 (t, *J* = 7.5 Hz, 2H), 8.35 (d,  
52  
53 *J* = 8.5 Hz, 2H), 8.55 (m, 2H), 8.68 (d, *J* = 9 Hz, 2H), 8.95 (d, *J* = 9.5 Hz, 2H); <sup>13</sup>C NMR (125.7  
54  
55 MHz, DMSO-d<sub>6</sub>): δ=119.9, 122.3, 122.7, 124.1, 127.5, 128.1, 129, 129.8, 137.1, 139.2, 141.9,  
56  
57  
58  
59  
60

1  
2  
3 145.3, 146.5, 146.9, 150.1, 163.3; HRMS FAB (m/z) calculated for C<sub>27</sub>H<sub>19</sub>N<sub>2</sub>O<sub>4</sub> [M]<sup>+</sup> 435.1345;  
4  
5 found 435.1343.  
6  
7

8 **[1,1':4',1''-Terphenyl]-4-yl 10-methyl-10λ<sup>4</sup>-acridine-9-carboxylate, trifluoromethane-**  
9 **sulfonate salt (26).** Yellow solid (0.04 g, 6%); mp 279–282 °C; <sup>1</sup>H NMR (500 MHz, DMSO-  
10 d<sub>6</sub>): δ 4.97 (s, 3H), 7.39 (t, *J* = 7.5 Hz, 1H), 7.49 (t, *J* = 8 Hz, 2H), 7.74 (d, *J* = 7 Hz, 2H), 7.82 (d,  
11 *J* = 8 Hz, 2H), 7.87 (d, *J* = 9 Hz, 4H), 7.98 (d, *J* = 8.5 Hz, 2H), 8.18 (t, *J* = 8.5 Hz, 2H), 8.55 (t, *J*  
12 = 8 Hz, 2H), 8.68 (d, *J* = 8.5 Hz, 2H), 8.95 (d, *J* = 9.5 Hz, 2H); <sup>13</sup>C NMR (125.7 MHz, DMSO-  
13 d<sub>6</sub>): δ 112.9, 119.9, 121.3, 122.3, 122.4, 123.5, 126.5, 126.6, 126.9, 127, 127.1, 127.2, 127.4,  
14 127.5, 127.6, 128.2, 128.9, 129, 129.1, 129.8, 137.9, 138.9, 139.2, 139.4, 139.5, 141.9, 146.7,  
15 149, 163.5; HRMS FAB (m/z) calculated for C<sub>33</sub>H<sub>24</sub>NO<sub>2</sub> [M]<sup>+</sup> 466.1807; found 466.1807.  
16  
17  
18  
19  
20  
21  
22  
23  
24  
25  
26  
27  
28  
29

30 **Chemiluminescence Measurement of Compounds 1–26.** Chemiluminescence was  
31 measured using a Lumat LB 9507 (Berthold, Bad Wildbad, Germany) luminometer.  
32  
33

34  
35 To 50 μL of a 10 nM solution of compounds 1–26 in dimethyl sulfoxide was added 100 μL of  
36 a buffer solution (100 mM Tris-HCl for pH 7 and pH 8, 100 mM Gly-NaOH for pH 9 and pH  
37 10). After allowing the mixture to stand for 20 s, the CL reaction was initiated by adding 100  
38 μL of 5–100 mM aqueous hydrogen peroxide solution to the luminometer using an automatic  
39 injection system. The CL emission was measured for 1 min and the integral photon counts were  
40 used to evaluate the CL intensity.  
41  
42  
43  
44  
45  
46  
47  
48

49 **Standard Curves for Hydrogen Peroxide at pH 7 and pH 8 using Compounds 3, 4 and 13.**

50  
51 To 50 μL of a 10 nM solution of compound 3, compound 4 or compound 13 in dimethyl  
52 sulfoxide was added 100 μL of a buffer solution (100 mM Tris-HCl for pH 7 and pH 8). After  
53 allowing the mixture to stand for 20 s, the CL reaction was initiated by adding 100 μL of 0–40  
54  
55  
56  
57  
58  
59  
60

1  
2  
3 mM aqueous hydrogen peroxide solution to the luminometer using an automatic injection system.  
4  
5 The CL emission was measured for 1 min and the integral photon counts were used to evaluate  
6  
7 the CL intensity.  
8  
9

10 **Chemical Stability of Compounds 1, 3, 4 and 10–13.** A 10 nM dimethyl sulfoxide solution  
11  
12 of compounds 1, 3, 4 and 10–13 was allowed to stand at 25 °C for 3 h. Then, to 50 μL of the 10  
13  
14 nM dimethyl sulfoxide solution of compounds 1, 3, 4 and 10–13 was added 100 μL of a buffer  
15  
16 solution (100 mM Tris-HCl, pH 7). After allowing this mixture to stand for 20 s, the CL  
17  
18 reaction was initiated by adding 100 μL of 5 mM aqueous hydrogen peroxide solution to the  
19  
20 luminometer using an automatic injection system. The CL emission was measured for 1 min  
21  
22 and the integral photon counts were used to evaluate the CL intensity.  
23  
24  
25  
26

27 **Standard Curves for Glucose using Compound 13.** To 250 μL of 10–2000 μM glucose in  
28  
29 100 mM phosphate buffer (pH 7.5) was added 250 μL of a glucose oxidase (1 U) in 100 mM  
30  
31 phosphate buffer (pH 7.5). The reaction mixture was incubated at 37 °C for 10 min and 100 μL  
32  
33 of the mixture solution was initiated by adding 100 μL of 10 nM compound 13 in dimethyl  
34  
35 sulfoxide to the luminometer using an automatic injection system. The CL emission was  
36  
37 measured for 1 min and the integral photon counts were used to evaluate the CL intensity.  
38  
39  
40  
41

42 **Computational Method.** Molecular structures of two compounds (1 and 3) and the correlated  
43  
44 molecules were fully optimized using the density functional theory (DFT) at Becke and Lee,  
45  
46 Yang, and Parr (B3LYP)<sup>67,68</sup> and Zhao and Truhlar (M06-X2)<sup>69</sup> levels of theory. Dunning's cc-  
47  
48 pVDZ basis set was used.<sup>61</sup> Energy minima were verified by vibrational frequency analysis. To  
49  
50 determine the energy diagram on the proposed CL reaction,<sup>45,46a</sup> the polarizable continuum  
51  
52 model (PCM) was employed; the solution was dimethyl sulfoxide. Symmetry adapted cluster /  
53  
54 configuration interaction (SAC-CI) method was employed to confirm and search the  
55  
56  
57  
58  
59  
60

1  
2  
3 electronically excited states by a single-point calculation with DFT optimized geometries on  
4  
5 PCM models. Almost all of these *ab initio* calculations were performed with use of the  
6  
7 electronic structure program Gaussian 09.<sup>70</sup> Using 8 cpu-cores of AMD Opteron 2382 and 8 GB  
8  
9 ram (Tempest9D2 model, CONCURRENT SYSTEM ltd.) in Sophia University, it took about  
10  
11 four months to obtain all results. However, spin-orbit coupling elements were obtained by  
12  
13 complete active space (CAS) SCF methods at cc-pVDZ basis set. The active space was  
14  
15 determined by (6e, 4o).  
16  
17  
18  
19  
20  
21

## 22 **Supporting Information**

23  
24  
25 The Supporting Information is available free of charge on the ACS Publications website at  
26  
27 DOI: .  
28

29  
30  
31 <sup>1</sup>H and <sup>13</sup>C NMR spectra and computational data tables  
32  
33  
34  
35

## 36 **Notes**

37  
38  
39 The authors declare no competing financial interest.  
40  
41  
42  
43  
44

## 45 **ACKNOWLEDGMENTS**

46  
47 This work was performed as part of a Cooperative Research Program of the “Network Joint  
48  
49 Research Center for Materials and Devices.”  
50  
51  
52  
53  
54

## 55 **REFERENCES**

1  
2  
3  
4 (1) (a) Kricka, L. J. *Anal. Chem.* **1995**, *67*, 499R–502R. (b) Kricka, L. J. *Anal. Chem.* **1999**,  
5  
6 *71*, 305R–308R. (c) Kricka, L. J. *Anal. Chim. Acta* **2003**, *500*, 279–286. (d) Kricka, L. J.;  
7  
8 Voyta, J. C.; Bronstein, I. *Methods Enzymol.* **2000**, *305*, 370–390. (e) Park, J. Y.; Kim, T. J.;  
9  
10 Artis, D.; Waldman, S. A.; Kricka, L. J. *Luminescence* **2010**, *25*, 463–465. (f) Park, J. Y.;  
11  
12 Gunpat, J.; Liu, L.; Edwards, B.; Christie, A.; Xie, X-J.; Kricka, L. J.; Mason, R. P.  
13  
14 *Luminescence* **2014**, *29*, 553–558.  
15  
16

17  
18  
19 (2) (a) Honda, K.; Imai, K. *Anal. Chem.* **1983**, *55*, 940–943. (b) Tsunoda, M.; Takezawa, K.;  
20  
21 Imai, K. *Analyst* **2001**, *126*, 637–640. (c) Tsunoda, M.; Imai, K. *Anal. Chim. Acta* **2005**, *541*,  
22  
23 13–23.  
24  
25

26  
27  
28 (3) (a) Shimomura, O.; Wu, C.; Murai, A.; Nakamura, H. *Anal. Biochem.* **1998**, *258*, 230–235.  
29  
30 (b) Shimomura, O.; Teranishi, K. *Luminescence* **2000**, *15*, 51–58.  
31  
32

33  
34 (4) (a) Nakazono, M.; Hino, T.; Zaitzu, K. *J. Photochem. Photobiol. A Chem.* **2007**, *186*,  
35  
36 99–105. (b) Nakazono, M.; Nanbu, S.; Uesaki, A.; Kuwano, R.; Kashiwabara, M.; Zaitzu, K.  
37  
38 *Org. Lett.* **2007**, *9*, 3583–3586. (c) Agawa, H.; Nakazono, M.; Nanbu, S.; Zaitzu, K. *Org. Lett.*  
39  
40 **2008**, *10*, 5171–5174. (d) Nakazono, M.; Jinguji, A.; Nanbu, S.; Kuwano, R.; Zheng, Z.; Saita,  
41  
42 K.; Oshikawa, Y.; Mikuni, Y.; Murakami, T.; Zhao, Y.; Sasaki, S.; Zaitzu, K. *Phys. Chem. Chem.*  
43  
44 *Phys.* **2010**, *12*, 9783–9793.  
45  
46  
47

48  
49 (5) (a) Kuroda, N.; Shimoda, R.; Wada, M.; Nakashima, K. *Anal. Chim. Acta* **2000**, *403*,  
50  
51 131–136. (b) Wada, M.; Abe, K.; Ikeda, R.; Harada, S.; Kuroda, N.; Nakashima, K. *Talanta*  
52  
53 **2010**, *81*, 1133–1136. (c) Elgawish, M. S.; Shimomai, C.; Kishikawa, N.; Ohyama, K.;  
54  
55 Nakashima, K.; Kuroda, N. *Analyst* **2012**, *137*, 4802–4808.  
56  
57  
58  
59  
60

1  
2  
3 (6) (a) Arakawa, H.; Maeda, M.; Tsuji, A. *Anal. Biochem.* **1991**, *199*, 238–242. (b) Arakawa,  
4 H.; Kanemitsu, M.; Tajima, N.; Maeda, M. *Anal. Chim. Acta* **2002**, *472*, 75–82. (c) Arakawa,  
5 H.; Masuda, K.; Tajima, N.; Maeda, M. *Luminescence* **2007**, *22*, 245–250.

10  
11 (7) (a) Roda, A.; Pasini, P.; Mirasoli, M.; Michelini, E.; Guardigli, M. *Trends Biotechnol.*  
12 **2004**, *22*, 295–303. (b) Roda, A.; Di Fusco, M.; Quintavalla, A.; Guardigli, M.; Mirasoli, M.;  
13 Lombardo, M.; Trombini, C. *Anal. Chem.* **2012**, *84*, 9913–9919. (c) Di Fusco, M.; Quintavalla,  
14 A.; Trombini, C.; Lombardo, M.; Roda, A.; Guardigli, M.; Mirasoli, M. *J. Org. Chem.* **2013**, *78*,  
15 11238–11246. (d) Roda, A.; Michelini, E.; Cevenini, L.; Calabria, D.; Calabretta, M. M.;  
16 Simoni, P. *Anal. Chem.* **2014**, *86*, 7299–7304. (e) Roda, A.; Guardigli, M.; Calabria, D.;  
17 Calabretta, M. M.; Cevenini, L.; Michelini, E. *Analyst* **2014**, *139*, 6494–6501.

22  
23 (8) (a) Huang, G.; Lv, Y.; Zhang, S.; Yang, C.; Zhang, X. *Anal. Chem.* **2005**, *77*, 7356–7365.  
24  
25 (b) Wang, W.; Lu, Y.; Zhang, S.; Wang, S.; Cao, P.; Tian, Y.; Zhang, X. *Luminescence* **2009**,  
26 *24*, 55–61. (c) Niu, W.; Kong, H.; Wang, H.; Zhang, Y.; Zhang, S.; Zhang, X. *Anal. Bioanal.*  
27 *Chem.* **2012**, *402*, 389–395.

28  
29 (9) Teranishi, K.; Nishiguchi, T. *Anal. Biochem.* **2007**, *352*, 185–195.

30  
31 (10) (a) Zhang, H.; Smanmoo, C.; Kabashima, T.; Lu, J.; Kai, M. *Angew. Chem. Int. Ed.* **2007**,  
32 *46*, 8226–8229. (b) Xin, L.; Cao, Z.; Lau, C.; Kai, M.; Lu, J. *Luminescence* **2010**, *25*, 336–342.  
33  
34 (c) El-Mahdy, A. F. M.; Shibata, T.; Kabashima, T.; Kai, M. *Chem. Commun.* **2014**, 859–861.

35  
36 (11) Zhang, Y.; Tan, C.; Fei, R.; Liu, X.; Zhou, Y.; Chen, J.; Chen, H.; Zhou, R.; Hu, Y. *Anal.*  
37 *Chem.* **2014**, *86*, 1115–1122.

- 1  
2  
3  
4 (12) White, E. H.; Roswell, D. F. *Acc. Chem. Res.* **1970**, *3*, 54–62.  
5  
6  
7 (13) Nakazono, M., Nohta, H.; Sasamoto, K.; Ohkura, Y. *Anal. Sci.* **1992**, *8*, 779–783.  
8  
9  
10 (14) Zhao, J-Y.; Labbe, J.; Dovichi, N. J. *J. Microcolumn Sep.* **1993**, *5*, 331–339.  
11  
12  
13 (15) Tsukagoshi, K.; Nakamura, T.; Nakajima, R. *Anal. Chem.* **2002**, *74*, 4109–4116.  
14  
15  
16  
17 (16) Huang, G.; Ouyang, J.; Delanghe, J. R.; Baeyens, W. R. G.; Dai, Z. *Anal. Chem.* **2004**, *76*,  
18  
19 2997–3004.  
20  
21  
22 (17) Erwen, M.; Burgess, K. *Angew. Chem. Int. Ed.* **2007**, *46*, 1684–1687.  
23  
24  
25  
26 (18) Qi, Y.; Li, B. *Chem. Eur. J.* **2011**, *17*, 1642–1648.  
27  
28  
29 (19) Bailey, T. S.; Pluth, M. D. *J. Am. Chem. Soc.* **2013**, *135*, 16697–16704.  
30  
31  
32  
33 (20) He, Y. Cui, H. *Chem. Eur. J.* **2013**, *19*, 13584–13589.  
34  
35  
36 (21) Griesbeck, A. G.; Diaz-Miara, Y.; Fichtler, R.; Jacobi Von Wangelin, A.; Pérez -Ruiz, R.;  
37  
38 Sampedro, D. *Chem. Eur. J.* **2015**, *21*, 9975–9979.  
39  
40  
41  
42 (22) Ruberto, M. A.; Grayeski, M. L. *Anal. Chem.* **1992**, *64*, 2758–2762.  
43  
44  
45 (23) Sato, N. *Tetrahedron Lett.* **1996**, *37*, 8519–8522.  
46  
47  
48 (24) Razavi, Z.; McCapra, F. *Luminescence* **2000**, *15*, 245–249.  
49  
50  
51  
52 (25) Renotte, R.; Sarlet, G.; Thunus, L.; Lejeune, R. *Luminescence* **2000**, *15*, 311–320.  
53  
54  
55 (26) King, D. W.; Cooper, W. J.; Rusak, S. A.; Peake, B. M.; Kiddle, J. J.; O’Sullivan, D. W.;  
56  
57 Melamed, M. L.; Morgan, C. R.; Theberge, S. M. *Anal. Chem.* **2007**, *79*, 4169–4176.  
58  
59  
60

- 1  
2  
3 (27) Krzymiński, K.; Roshal, A. D.; Niziołek, A. *Spectrochim. Acta Part A*. **2008**, *70*, 394–  
4  
5 402.  
6  
7  
8  
9 (28) Smith, K.; Yangb, J.-J.; Li, Z.; Weeks, I.; Woodhead, J. S. *J. Photochem. Photobiol. A*  
10  
11 *Chem.* **2009**, *203*, 72–79.  
12  
13  
14 (29) Browne, K. A.; Deheyn, D. D.; El-Hiti, G. A.; Smith, K.; Weeks, I. *J. Am. Chem. Soc.*  
15  
16 **2011**, *133*, 14637–14648.  
17  
18  
19  
20 (30) (a) Natrajan, A.; Sharpe, D. *Org. Biomol. Chem.* **2013**, *1*, 1026–1039. (b) Wang, S.;  
21  
22 Natrajan, A. *RSC Adv.* **2015**, *5*, 19989–20002.  
23  
24  
25  
26 (31) Waldemar, A.; Wilhelm, J. B. *Angew. Chem. Int. Ed.* **1984**, *23*, 166–167.  
27  
28  
29  
30 (32) Schaap, A. P.; Sandison, M. D.; Handley, R. S. *Tetrahedron Lett.* **1987**, *11*, 1159–1162.  
31  
32  
33  
34 (33) Bronstein, I.; Edwards, B.; Voyta, J. C. *J. Biolumin. Chemilumin.* **1989**, *4*, 99–111.  
35  
36  
37 (34) (a) Matsumoto, M.; Suzuki, H.; Watanabe, N.; Ijuin, H. K.; Tanaka, J.; Tanaka, C. *J. Org.*  
38  
39 *Chem.*, **2011**, *76*, 5006–5017. (b) Tanimura, M.; Watanabe, N.; Ijuin, H. K.; Matsumoto, M. *J.*  
40  
41 *Org. Chem.* **2012**, *77*, 4725–4731.  
42  
43  
44 (35) Chen, Y.; Spiering, A. J. H.; Karthikeyan, S.; Peters, G. W. M.; Meijer, E. W.; Sijbesma,  
45  
46 R. P. *Nat. Chem.* **2012**, *4*, 559–562.  
47  
48  
49  
50 (36) Kawashima, H.; Watanabe, N.; Ijuin, H. K.; Matsumoto, M. *Luminescence* **2013**, *28*,  
51  
52 696–704.  
53  
54  
55  
56  
57  
58  
59  
60

1  
2  
3 (37) Fusco, M. D.; Quintavalla, A.; Trombini, C.; Lombardo, M.; Roda, A.; Guardigli, M.;  
4  
5 Mirasoli, M. *J. Org. Chem.* **2013**, *78*, 11238–11246.

6  
7  
8  
9 (38) Zhang, N.; Francis, K. P.; Prakash, A.; Ansaldi, D. *Nat. Med.* **2013**, *19*, 500–505.

10  
11  
12 (39) (a) Weeks, I.; Beheshti, I.; McCapra, F.; Campbell, A. K.; Woodhead, J. S. *Clin. Chem.*  
13 **1983**, *29*, 1474–1479. (b) Natrajan, A.; Sharpe, D.; Costello, J.; Jiang, Q. *Anal. Biochem.* **2010**,  
14 *406*, 204–213. (c) Natrajan, A.; Sharpe, D.; Wen, D. *Org. Biomol. Chem.* **2012**, *10*, 3432–3447.

15  
16  
17  
18 (40) Arakawa, H.; Tsuruoka, K.; Ohno, K.; Tajima, N.; Nagano, H. *Luminescence* **2014**, *29*,  
19  
20  
21  
22 374–377.

23  
24  
25 (41) Wang, W.; Ouyang, H.; Yang, S.; Wang, L.; Fu, Z. *Analyst* **2015**, *140*, 1215–1220.

26  
27  
28  
29 (42) (a) Ciscato, L. F. M. L.; Bartoloni, F. H.; Weiss, D.; Beckert, R.; Baader, W. J. *J. Org.*  
30  
31  
32 *Chem.* **2010**, *75*, 6574–6580. (b) Maruyama, T.; Sugishita, H.; Kujira, H.; Ichikawa, M.; Hattori,  
33  
34  
35 Y.; Motoyoshiya, J. *Tetrahedron Lett.* **2013**, *54*, 1338–1343.

36  
37  
38 (43) Turan, I. S.; Akkaya, E. U. *Org. Lett.* **2014**, *16*, 1680–1683.

39  
40  
41 (44) (a) Schramm, S.; Weiss, D.; Navizet, I.; Roca-Sanjuán, D.; Beckert, R.; Görls, H.  
42  
43 *ARKIVOC* **2013**, *3*, 174–188. (b) Ciscato, L. F. M. L.; Bartoloni, F. H.; Colavite, A. S.; Weiss,  
44  
45  
46 D.; Beckert, R.; Schramm, S. *Photochem. Photobiol. Sci.* **2014**, *13*, 32–37. (c) Schramm, S.;  
47  
48 Ciscato, L. F. M. L.; Oesau, P.; Krieg, R.; Richter, J. F.; Navizet, I.; Roca-Sanjuan, D.; Weiss,  
49  
50  
51 D.; Beckert, R. *ARKIVOC* **2015**, *5*, 44–59. (d) Schramm, S.; Navizet, I.; Naumov, P.; Nath, N.  
52  
53  
54 K.; Berraud-Pache, R.; Oesau, P.; Weiss, D.; Beckert, R. *Eur. J. Org. Chem.* **2016**, *2016*,  
55  
56  
57 678–681.

1  
2  
3 (45) McCapra, F.; Richardson, D. G.; Chang, Y. C. *Photochem. Photobiol.* **1965**, *4*,  
4  
5  
6 1111–1121.

7  
8  
9 (46) (a) Nelson, N. C.; Cheikh, A. B.; Matsuda, E.; Becker, M. M. *Biochemistry* **1996**, *35*,  
10  
11 8429–8438. (b) Nelson, N. C.; Woodhead, J. S.; Weeks, I.; Cheikh, A. B. Eur. Pat. Appl.  
12  
13 (1996). EP 709466 A2 19960501.

14  
15  
16  
17 (47) Wang, Z.; Yue, H.; Wang, Y.; Wang, L.; Fu, Z. *Electrophoresis* **2014**, *35*, 1000–1003.

18  
19  
20 (48) Brown, R. C.; Weeks, I.; Fisher, M.; Harbron, S.; Taylorson, C. J.; Woodhead, J. S. *Anal.*  
21  
22 *Biochem.* **1998**, *259*, 142–151.

23  
24  
25  
26 (49) Brown, R. C.; Li, Z.; Rutter, A. J.; Mu, X.; Weeks, O. H.; Smith, K.; Weeks, I. *Org.*  
27  
28 *Biomol Chem.* **2009**, *7*, 386–394.

29  
30  
31  
32 (50) Trzybiński, D.; Skupień, M.; Krzywiński, K.; Sikorski, A.; Błażejowski, J. *Acta. Crystl.*  
33  
34 **2009**, *E65*, o770–o771.

35  
36  
37  
38 (51) David-Cordonnier, M-H.; Hildebrand, M-P.; Baldeyrou, B.; Lansiaux, A.; Keuser, C.;  
39  
40 Benzschawel, K.; Lemster, T.; Pindur, U. *Eur. J. Med. Chem.* **2007**, *42*, 752–771.

41  
42  
43 (52) Moteki, S. A.; Takacs, J. M. *Angew. Chem. Int. Ed.* **2008**, *47*, 894–897.

44  
45  
46  
47 (53) Ince, M.; Gartmann, N.; Claessens, C. G.; Torres, T.; Brühwiler, D. *Org. Lett.* **2011**, *13*,  
48  
49 4918–4921.

50  
51  
52 (54) McCapra, F. *Acc. Chem. Res.* **1976**, *9*, 201–208.

53  
54  
55 (55) The pKa values of phenols were obtained from a document entitled *pKa Data Compiled*  
56  
57  
58  
59  
60

1  
2  
3 by R. Williams.  
4

5  
6 (56) Krzymiński, K.; Ożóg, A.; Malecha, P.; Roshal, A. D.; Wróblewska, A.; Zadykowicz,  
7  
8 B.; Błażejowski, J. *J. Org. Chem.* **2011**, *76*, 1072–1085.  
9

10  
11 (57) Economou, A.; Panoutsou, P.; Themelis, D. G. *Anal. Chim. Acta* **2006**, *572*, 140–147.  
12

13  
14 (58) Shiang, T-C.; Huang, C-C.; Chang, H-T. *Chem. Commun.* **2009**, 3437–3439.  
15

16  
17 (59) Khajvand, T.; Alijanpour, O.; Chaichi, M. J.; Vafaezadeh, M.; Hashemi, M. M. *Anal.*  
18  
19 *Bioanal. Chem.* **2015**, *407*, 6127–6136.  
20

21  
22 (60) Rak, J.; Skurski, P.; Błażejowski, J. *J. Org. Chem.* **1999**, *64*, 3002–3008.  
23

24  
25 (61) Dunning, T. H. *J. Chem. Phys.* **1989**, *90*, 1007–1023.  
26

27  
28 (62) Gundermann, K. D.; McCapra, F. *Chemiluminescence in Organic Chemistry*, Springer  
29  
30 Verlag, Berlin, Heidelberg, New York, **1987**.  
31

32  
33 (63) Nakamura, H. *Nonadiabatic Transition: Concepts, Basic Theories and Applications*, 2<sup>nd</sup>  
34  
35 revised ed., World Scientific, Singapore, **2012**.  
36

37  
38 (64) Werner, H.-J.; Knowles, P. J.; Knizia, G.; Manby, F. R.; Schütz, M.; Celani, P.; Györffy,  
39  
40 W.; Kats, D.; Korona, T.; Lindh, R.; Mitrushenkov, A.; Rauhut, G.; Shamasundar, K. R.; Adler,  
41  
42 T. B.; Amos, R. D.; Bernhardsson, A.; Berning, A.; Cooper, D. L.; Deegan, M. J. O.; Dobbyn, A.  
43  
44 J.; Eckert, F.; Goll, E.; Hampel, C.; Hesselmann, A.; Hetzer, G.; Hrenar, T.; Jansen, G.; Köppl,  
45  
46 C.; Liu, Y.; Lloyd, A. W.; Mata, R. A.; May, A. J.; McNicholas, S. J.; Meyer, W.; Mura, M. E.;  
47  
48 Nicklaß, A.; O'Neill, D. P.; Palmieri, P.; Peng, D.; Pflüger, K.; Pitzer, R.; Reiher, M.; Shiozaki,  
49  
50  
51  
52  
53  
54  
55  
56  
57  
58  
59  
60

1  
2  
3 T.; Stoll, H.; Stone, A. J.; Tarroni, R.; Thorsteinsson, T.; Wang, M. Version 2012.1 (see  
4  
5  
6 <http://www.molpro.net>).

7  
8  
9 (65) (a) Kobayashi, T.; Kuramochi, H.; Harada, Y.; Suzuki, Y.; Ichimura, T. *J. Phys. Chem. A*  
10  
11 **2009**, *113*, 12088–12093. (b) Kobayashi, T.; Kuramochi, H.; Suzuki, Y.; Ichimura, T. *Phys.*  
12  
13 *Chem. Chem. Phys.* **2010**, *12*, 5140–5148. (c) Kuramochi, H.; Kobayashi, T.; Suzuki, Y.;  
14  
15 Ichimura, T. *J. Phys. Chem. B* **2010**, *114*, 8782–8789.

16  
17  
18  
19 (66) Radzig A. A.; Smirnov B. M. *Springer Series in Chemical Physics, Reference data on*  
20  
21 *atoms, molecules and ions*, Springer **1985**.

22  
23  
24  
25 (67) Becke, A. D. *J. Chem. Phys.* **1993**, *98*, 5648–5652.

26  
27  
28 (68) Lee, C. T.; Yang, W. T.; Parr, R. G. *Phys. Rev. B* **1988**, *37*, 785–789.

29  
30  
31 (69) Zhao, Y.; Truhlar, D. G. *Theor. Chem. Acc.* **2008**, *120*, 215–241.

32  
33  
34 (70) Gaussian 09, Revision D.01, Frisch, M. J.; Trucks, G. W.; Schlegel, H. B.; Scuseria,  
35  
36 G. E.; Robb, M. A.; Cheeseman, J. R.; Scalmani, G.; Barone, V.; Mennucci, B.; Petersson, G. A.;  
37  
38 Nakatsuji, H.; Caricato, M.; Li, X.; Hratchian, H. P.; Izmaylov, A. F.; Bloino, J.; Zheng, G.;  
39  
40 Sonnenberg, J. L.; Hada, M.; Ehara, M.; Toyota, K.; Fukuda, R.; Hasegawa, J.; Ishida, M.;  
41  
42 Nakajima, T.; Honda, Y.; Kitao, O.; Nakai, H.; Vreven, T.; Montgomery, J. A.; Peralta, Jr., J. E.;  
43  
44 Ogliaro, F.; Bearpark, M.; Heyd, J. J.; Brothers, E.; Kudin, K. N.; Staroverov, V. N.; Kobayashi,  
45  
46 R.; Normand, J.; Raghavachari, K.; Rendell, A.; Burant, J. C.; Iyengar, S. S.; Tomasi, J.; Cossi,  
47  
48 M.; Rega, N.; Millam, J. M.; Klene, M.; Knox, J. E.; Cross, J. B.; Bakken, V.; Adamo, C.;  
49  
50 Jaramillo, J.; Gomperts, R.; Stratmann, R. E.; Yazyev, O.; Austin, A. J.; Cammi, R.; Pomelli, C.;  
51  
52 Ohterski, J. W.; Martin, R. L.; Morokuma, K.; Zakrzewski, V. G.; Voth, G. A.; Salvador, P.;

1  
2  
3 Dannenberg, J. J.; Dapprich, S.; Daniels, A. D.; Farkas, Ö.; Foresman, J. B.; Ortiz, J. V.;  
4  
5  
6 Cioslowski, J.; Fox, D. J. Gaussian, Inc., Wallingford CT, **2009**.  
7  
8  
9  
10  
11  
12  
13  
14  
15  
16  
17  
18  
19  
20  
21  
22  
23  
24  
25  
26  
27  
28  
29  
30  
31  
32  
33  
34  
35  
36  
37  
38  
39  
40  
41  
42  
43  
44  
45  
46  
47  
48  
49  
50  
51  
52  
53  
54  
55  
56  
57  
58  
59  
60